REPUBLIC OF TURKEY
ACIBADEM MEHMET ALI AYDINLAR UNIVERSITY
INSTITUTE OF NATURAL AND APPLIED SCIENCES

EVALUATION OF BEST PREPROCESSING PRACTICES FOR DENOISING FNIRS SIGNALS COLLECTED DURING COGNITIVE AND MOTOR TASKS

Umut KARADENİZ
DEPARTMENT OF MEDICAL ENGINEERING

SUPERVISOR
Asst. Prof. Sinem Burcu Erdoğan

ISTANBUL – 2020

DECLARATION

I declare that the works and information contained in this thesis are my own except where explicitly stated otherwise in the text. I am fully aware of all the ethical rules and there is not any violation of copyright and any kind of patent.

11/12/2019

Umut Karadeniz

ACKNOWLEDGEMENTS

First of all, I would like to thank my supervisor, Asst. Prof. Sinem Burcu Erdoğan, who has always supported since my acceptance to the M.Sc program and she was always there whenever or whatever I need. She steered me in the right direction, motivated and continuously encouraged me during my Masters education.

I am also very grateful to my beloved friends Ibrahim Mert Capacı, Begüm Yalçın and Lisa Kobayashi Frisk. Their passionate participation, comments, knowledge and motivation during the completion of this thesis has given me great motivation and inspiration throughout this period.

TABLE OF CONTENTS

Page

LIST OF FIGURES

Page

LIST OF SYMBOLS & ABBREVIATIONS

FNIRS	Functional Near-Infrared Spectroscopy
3D	Three-Dimensional
EEG	Electroencephalography
ACU	Acıbadem Mehmet Ali Aydınlar University
BCI	Brain-Computer Interface
ROI	Regions of Interest
MEG	Magnetoencephalography
NVC	Neurovascular Coupling
Cm	Centimeter
CBF	Cerebral Blood Flow
HBO	Oxyhemoglobin
HBT	Total Hemoglobin
PCA	Principle Component Analysis
ICA	Independent Component Analysis

LF	Low Frequency
CW	Continuous Wave
MBLL	Modified Beer-Lambert Law
FIR	Finite Impulse Response
BP	Bandpass
LP	Low Pass
HP	High Pass
FFT	Fast Fourier Transform
CBSI	Correlation-Based Signal Improvement
SPM	Statistical Parametric Mapping
SNR	Signal-To-Noise Ratio SNR
GLM	General Lineer Model
Fc	Cut-Off Frequencies
BOLD	Blood Oxygen Level Dependent

SUMMARY

Over the past two decades, FNIRS has become a practical and effective neuroimaging tool for investigating functional organization and specialization of the human brain. FNIRS systems have gained increasing popularity in neuroscience research due to non-invasive and light weight configuration and designs, field deployability, quick set-up time and planning. However, a major problem with FNIRS recordings has been the presence of various sources of noise mainly due to systemic physiological, experimental and instrumental artifacts. While instrumental noise can be eliminated by digital filters, a critical portion of the frequency spectrum of physiological effects caused by variations in heartbeat, blood pressure, respiratory activity and vascular tone overlap with that of the neuronally induced hemodynamic signals of interest. The presence of such systemic fluctuations degrades the signal to noise ratio by introducing false positive and false negatives besides real time interpretability of the signals. While many studies have emphasized the severity of physiological noise, no golden standard preprocessing technique could be proposed for eliminating systemic physiological artifacts which overlay hemodynamic signals induced by neuronal activation. Several methods for removal of systemic and motion artifacts from FNIRS signals have been proposed in the literature. However; no standardized pipeline of preprocessing steps could be reliably proposed as a gold standard for isolating the task related neuronally induced hemodynamic changes of interest. The aim of this study is to implement commonly applied noise reduction strategies in FNIRS literature into varying preprocessing pipelines and compare the performance of 48 different pipelines in increasing the signal to noise ratio in FNIRS signal collected during motor tasks.

Keywords: Functional near-infrared spectroscopy, Hemodynamic response, preprocessing, Denoising techniques, Motion correction, Band pass filtering, Low frequency noise removal

ÖZET

Bilişsel ve Motor Görevler Sırasında Toplanan İşlevsel Yakın Kızılaltı İşaretlerini Gürültüden Arındırmak Amacıyla Kullanılan En İyi Önişleme Tekniklerinin Değerlendirilmesi

Son yirmi yılda, işlevsel yakın kızılaltı spektroskopi (İYKAS), insan beyninin fonksiyonel organizasyonunu ve uzmanlığını araştırmak için pratik ve etkili bir beyin görüntüleme aracı haline gelmiştir. İYKAS sistemleri, non-invaziv ve kolay konfigürasyonu ve tasarımi ile, hızlı kurulum süresi ve planlanabilirligi nedeniyle sinirbilim araştırmalarında popülerlik kazanmıştır. Bununla birlikte, İYKAS çalışmalarında önemli bir sorun, sistemik fizyolojik, deneysel ve enstrümantal artefaktlar nedeniyle çeşitli gürültü kaynaklarının varlığı olmuştur. Enstrümantal gürültü dijital filtrelerle ortadan kaldırılabilirken, kalp atışı, kan basıncı, solunum aktivitesi ve vasküler tondaki değişikliklerin neden olduğu fizyolojik etkilerin frekans spektrumunun kritik bir kısmı, nöronal olarak indüklenen hemodinamik sinyallerinki ile örtüşmektedir. Bu tür sistemik dalgalanmaların varlığı, sinyallerin gerçek zamanlı incelenmesi sırasında yanlış pozitif ve yanlış negatifler ekleyerek sinyal-gürültü oranını bozar. Birçok çalışma fizyolojik gürültünün şiddetini vurgulasa da, nöronal aktivasyonun neden olduğu hemodinamik sinyalleri kaplayan sistemik fizyolojik artefaktları ortadan kaldırmak için hiçbir altın standart ön işleme tekniği henüz keşfedilmemiştir. Literatürde İYKAS sinyallerinden sistemik ve hareket artefaktlarının giderilmesi için çeşitli yöntemler önerilmiştir. Bu çalışmanın amacı, FNIRS literatüründe yaygın olarak uygulanan gürültü azaltma tekniklerini farklı önişleme standardlarında uygulamak ve toplanan İYKAS sinyalindeki sinyal / gürültü oranını artırmada 48 farklı filtre kombinasyonlarının performansını karşılaştırmaktır.

Anahtar Kelimeler: İşlevsel kizilötesine yakin spektroskopi sinyalleri, Hemodinamik fonksiyon, Ön işleme, Gürültü temizleme teknikleri, Hareket düzeltme, Bant geçiren filtreleme, Düşük frekanslı gürültü giderme

1. INTRODUCTION

Over the last two decades, functional near infrared spectroscopy (FNIRS) has emerged as a noninvasive and practical neuroimaging modality which provided neuroscientists and clinicians with a novel tool for studying changes in cerebral blood flow and tissue oxygenation during resting state and task conditions. FNIRS systems have gained increasing popularity in neuroscience research due to non-invasive and light weight configuration and designs, field deployability, quick set-up time and planning. However, a major problem with FNIRS recordings has been the presence of different sources of noise which are mainly due to systemic physiological, experimental and instrumental artifacts. Although many studies have focused on FNIRS and the physiological noise problem, there still does not exist a golden standard processing pipeline for removing systemic physiological and motion related artifacts.

The present study is dedicated to a very important question in FNIRS methodology, the development and validation of the best signal preprocessing techniques for removing systemic and physiological artifacts. Indeed, systemic contamination poses a severe problem by contributing to 20 to 30 % of the signal variance in both FNIRS and fMRI signals, hence strongly decreases the signal-to-noise ratio and can even lead to false positives and false negatives in detecting brain activation. While instrumental noise can be eliminated by digital filters, a critical portion of the frequency spectrum of physiological effects caused by variations in heartbeat, blood pressure, respiratory activity and vascular tone overlap with that of the neuronally induced hemodynamic signals of interest. The presence of such systemic fluctuations degrades the signal to noise ratio by introducing false positive and false negatives besides real time interpretability of the signals. Several methods for removal of systemic and motion artifacts from FNIRS signals have been proposed in the literature. However; no standardized pipeline of preprocessing steps could be reliably proposed as a gold standard for isolating the task related neuronally induced hemodynamic changes of interest.

The aim of this study is to combine the most commonly used noise reduction strategies for i) channel exclusion criteria, ii) motion artifact correction, iii) frequency filtering and iv) low frequency physiology removal into different preprocessing pipelines and compare the performance of 48 different pipelines in increasing the signal to noise ratio in FNIRS signal collected during motor tasks. The performance of each preprocessing pipeline is evaluated with the general linear model which is the most commonly used statistical method for modeling FNIRS and fMRI data.

The purpose of this study was to provide a visual reference showing the effects of different processing methods, to help inform researchers in setting up and evaluating a processing pipeline. We show the significant impact of pre- and post-processing choices. Optimum processing methods have not been established among FNIRS community, however in this study we propose a method for determining an active ROI depending on the type of experimental paradigm and channels used which would remain active after application of a majority of methods. Next, we evaluate the performance of 48 different pipelines on improving the signal quality in this ROI among all subject data. Our methodology presents a novel and practical automated selection for the best preprocessing practices for different NIRS data sets.

2. BACKGROUND

2.1. Functional Brain Imaging Techniques

Blood flow and brain oxygenation can be measured by functional brain imaging technologies. These techniques outcomes are often used together with structural imaging (e.g. MRI or CT). Tomography of positron emissions identify anomalies in brain tissues. The former measures anomalies by taking radiotracers into the brain, while the modality measures chemical changes of metabolite to define anomalies. The prospective role of functional MRI (fMRI) is to define the brain regions accountable for language, cognitive, and motor activity (sensorimotor cortex) instead of defining tissue defects. Magnetoencephalography tests electrical flow magnetic fields in the brain, detecting aberrant interaction. Magnetoencephalography can locate seizure foci and detect the cortex, visual cortex and auditory cortex of the sensorimotor. It is necessary to closely design and interpret functional neuroimaging research. Statistical analysis (often using a method called statistical parametric mapping) is often required in order to identify between the various causes of energy inside the brain. It could be particularly challenging once assessing procedures that are hard to conceptualize or are not linked with a readily definable function (e.g., belief and consciousness). The most common techniques for neuroimaging are explained below.

Electroencephalography (EEG)

EEG measures the electrical signals of neurons. EEG has the highest temporal resolution (>1000Hz) among the neuroimaging techniques (1). On the other hand, it has a very low spatial resolution (5-9 cm) (1). Due to the weak spatial resolution, localization of brain functions cannot be obtained. However, this issue is very significant for brain studies.

Brain-computer interface (BCI), psychology and neuroscience studies are the trending topics for EEG studies. In many experimental as well as medical studies, high-density EEG measurements have become common, given that most companies offer such devices easily and that the application of many electrodes has become fairly simple. Therefore, it is also not surprising that EEG source localization is progressive could be used to deduce the regions in the brain that induced the scalp activity (2). Continuous measurement of the scalp- and intracranial EEG is by far the most specific way to assess EEG source localization.

Due to its low resolution, each EEG inverse approach offers a source approximation for each voxel, which is a combination of the actual source values across all brain voxels. Commonly, this combining effect causes noticeable compression in source connectivity estimates based on inverse solutions. To reduce this deficiency, an unmixed approach is introduced for EEG inverse models based on piecewise approximation of the unnamed source through a brain segmentation formed by specified Regions of Interest (ROIs). The method is common and robust sufficient to be implemented with any defined ROI family, including point, surface, and 3D brain regions, to any reverse solution.

Magnetoencephalography (MEG)

Magnetoencephalography (MEG) monitors the magnetic fields produced throughout the brain by electrical currents. The values of the magnetic field are in the spectrum between Femto-tesla and pico-tesla. MEG gives the timing of neuronal activity with a very precise resolution. It is a non-invasive assessment. MEG is a precise measure of brain activity and its temporal resolution is very high. It also has a good spatial resolution (2-3 mm). For a good spatial viewpoint, MEG is generally coupled with a magnetic resonance imaging (MRI) brain. This MEG and MRI pairing are known as magnetic source imaging (MSI). (3) It is able to get information from the

magnetic fields of the body currents. Its temporal resolution is less than 1ms and on the other hand, it has few millimeters of spatial accuracy. In general, MEG is used for diagnosis of and localization of epilepsy activities and patients with brain tumors (3).

Magnetic resonance imaging (MRI)

Magnetic resonance imaging is a non-invasive imaging technique from which information about the structure and composition of different tissues can be obtained. fMRI is based on MRI, which in turn utilizes Nuclear Magnetic Resonance combined with magnetic field gradients to produce images that can integrate many distinct kinds of comparison such as T1 weighting, T2 weighting, flow, etc. In order to know the specific contrast technique primarily used in fMRI, brain metabolism needs to be discussed first. (4).

Functional Magnetic Resonance Imaging (fMRI) is a category of imaging techniques created to show spatial changes in brain metabolism over time (4). These metabolic modifications may lead to cognitive condition modifications caused by tasks or from uncontrolled procedures in the resting brain. Currently, functional magnetic resonance imaging (fMRI) can be accepted as a gold standard for brain mapping applications. Since it has high spatial accuracy and no ionizing radiation. However, it has low time resolution (1-3Hz) (1). Moreover, when fMRI measurement is implemented, the subject/patient should lie down on the MRI table during the measurements, all of which constitute additional weaknesses.

2.2. New Functional Imaging Era For Brain: Functional Near-Infrared Spectroscopy (FNIRS)

The number of functional neuroimaging studies conducted and published with functional near-infrared spectroscopy (FNIRS) has grown dramatically over the past few years (5). Basically, neurovascular coupling (NVC) connects the temporary neural activity with the associated rise in CBF. Neurovascular coupling corresponds to a correlation between alterations in local brain activity and alterations in local cerebral blood flow (CBF). CBF modifications in quantity and volume are closely linked to modifications in neuronal activity. (6) FNIRS measures changes in brain tissue concentration in oxyhemoglobin (HbO) and deoxyhemoglobin (HbR) related to increased brain metabolic demand during neuronal activity and increased tissue perfusion (7).

The advantages of FNIRS relative to other non-invasive neuroimaging methods such as EEG, fMRI or MEG include its mobility, prospective wearability, convenience of use, low purchasing and operating costs (especially when compared to fMRI and MEG), the spatial resolution of FNIRS relative to EEG, and better biochemical specificity (O2Hb relative to HbR) relative to fMRI. FNIRS measures temporal changes in relative concentrations of deoxyhemoglobin (HbR) and oxyhemoglobin (HbO) with respect to a baseline measurement and changes in total hemoglobin (HbT) with respect to time can be obtained from this data (8). Meanwhile, fMRI is only able to measure changes in HbR and blood flow. The range of FNIRS studies will continue to increase in the future exponentially.

When the historical development of NIRS is examined; Frans Jöbsis first worked in animal cells in 1977 with the in vivo NIRS method (9). Jöbsis enabled NIRS penetration using infrared light between 700-1000 nm on animal cells and performed cervical oxygenation changes during hyperventilation and visualized the induced

cerebral changes with NIRS. In 1984, David Delphy began to work on many types of NIRS devices. Three years later, Delphy first measured quantitative oxyhemoglobin, deoxyhemoglobin (total hemoglobin, cerebral blood volume and cerebral blood flow measurements in sick newborns. In 1985, Ferrari and Brazy performed the first clinical NIRS measurement in neonatal and adult cerebrovascular patients in separate studies. (9).

Specific applications vary from earlier diagnosis of cognitive or motor dysfunction in preterm babies, which possibly allow earlier operation while the brain still has strong plasticity, assessment of brain functions in children with unconscious intensive care, assessment of brain condition during surgery, identification of a stroke in the ambulance to psychiatric apps such as assessment (9).

Possibly very crucial is the reality that FNIRS is easy to deploy in theory, that it will not always be essential to have professional staff in the future with the field's continuous growth. Since FNIRS can be reconfigured and made wearable, this provides fresh areas of implementation, for example as a tool for providing fresh types of treatment for patients with severe stroke disabilities (11), leading to more efficient rehabilitation. It can also be used as a technique for providing neuro-feedback for fundamental neuroscientific research and/or therapeutic interventions (12). When the structural properties of FNIRS are examined, the features of each device vary.

For surface measurements, FNIRS is used as a neuroimaging method that includes optical dispersion technology and the measurement of hemodynamic changes in superficial tissues. The signal amplitude recorded in the optical dispersion measurements is determined by two factors: 1) light absorbed by the tissue, 2) light reflected back from the tissue. The diffuse optical measurements can acquire these changes and determine what these changes depend on. These absorption changes are predominantly determined by changes in hemoglobin concentration. The hemoglobin changes observed when the diffuse optical system is placed on the head measuring

brain activity. Brain activity may be related to different physiological events, and those events may cause changes in the optical features of neurons.

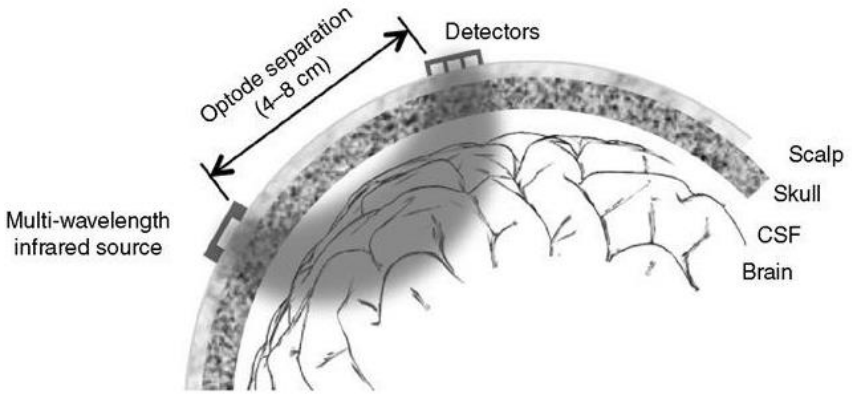

Figure 2.1. Light penetration in the human head (Banana shape).

Reference: Naseer N, Hong KS. FNIRS-based brain-computer interfaces: a review. Frontiers in human neuroscience. 2015 Jan 28;9:3.

In general, light source and light detector are placed at the surface of the subject's scalp (Figure 2.) Photons collected at the detector follow a banana shape from the light source and come from a depth of approximately one half the source-detector distance. The relative concentration of hemoglobin is calculated by using the modified Beer-Lambert law (mBLL). (14)

$$OD = -\log\frac{I}{Io} = \epsilon CLB + G \quad \text{(Eqn 2.1.)}$$

OD is the optical density value in the equation, Io displays incident light intensity and I is the light intensity identified and e is the chromophore's extinction coefficient. C is the concentration of the chromophore value, and L is the range between where the light enters the tissue and where the obtained material exits the tissue, B is a pathlength variable that accounts for rises in the tissue scattering photon pathlength, and G is a factor that accounts for the geometry of the test. We use the e log base convention. (14). Diffuse optical signals can be acquired in three main categories. These are continuous wave, frequency domain, and time-domain measurement.

Continuous Wave (CW) FNIRS

The Continuous Wave (CW) is commonly used in the FNIRS community. Basically, CW FNIRS measures stable light-emitting for tissue and detects how much light intensity tissue transmits. After relative blood volume and oxygenation changes in the brain tissues, meaningful information can be obtained.

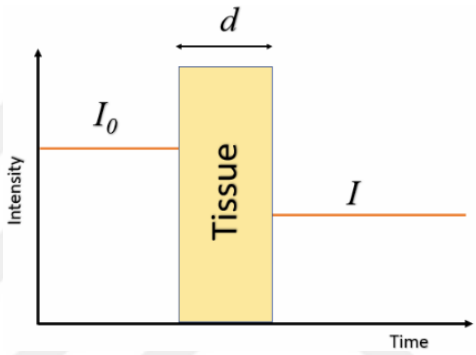

Figure 2.2. Continuous-wave.

Reference: Scholkmann F, Kleiser S, Metz AJ, Zimmermann R, Pavia JM, Wolf U, Wolf M. A review on continuous wave functional near-infrared spectroscopy and imaging instrumentation and methodology. Neuroimage. 2014 Jan 15;85:6-27

Hemoglobin molecules are the strongest absorbers and their absorption spectra characteristics can show temporal changes and important transient changes in interest moment scales (~ seconds).

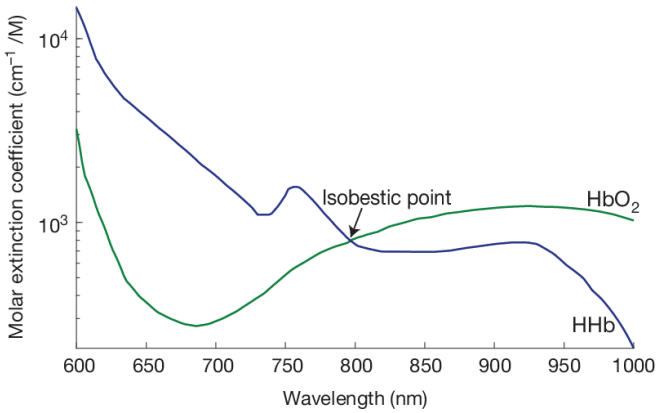

Figure 2.3. In the range between 600 and 1000 nm (infrared), the absorption spectrum of oxyhemoglobin and deoxyhemoglobin.

Reference: Ferrari M, Quaresima V. A brief review on the history of human functional near-infrared spectroscopy (FNIRS) development and fields of application. Neuroimage. 2012 Nov 1;63(2):921-35.

As shown in Figure 3, the two types of hemoglobin have distinct features of absorption. Oxyhemoglobin and deoxyhemoglobin absorb the same amount of light at the isosbestic point (about 800 nm) (9). In the measurement, relative changes in concentration with high reliability and contrast can be achieved from the background. on '~ seconds' time scale. It is, therefore, possible to extract their relative concentration shift from the background with elevated reliability and contrast (7).

Frequency Domain FNIRS

The light source is modulated in the radio frequency range (typically 100 MHz) in this method. At this point, the period between consecutive intensity peaks becomes similar to the moment constants to be regarded in tissue spectroscopy optical diffusion processes of optical properties and spatial sizes.

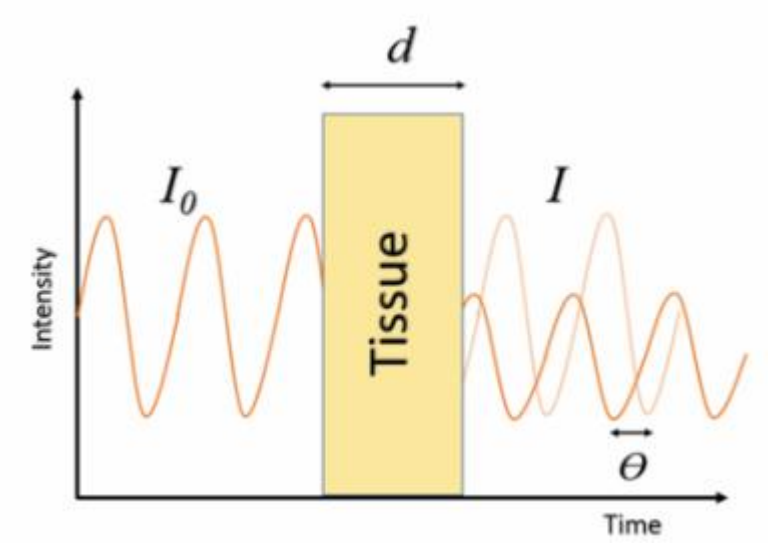

Figure 2.4. Frequency Domain.
Reference: Scholkmann F, Kleiser S, Metz AJ, Zimmermann R, Pavia JM, Wolf U, Wolf M. A review on continuous wave functional near-infrared spectroscopy and imaging instrumentation and methodology. Neuroimage. 2014 Jan 15;85:6-27

Especially, multiple scattering provides to effectively decrease the propagation velocity of photons over a specified distance to a fraction of the speed of light. Therefore, incoming light modulation creates propagating regions of high and low alternating photons. (7).

This can be defined as the propagation through the medium of 'Photon Density Waves'. Then, a detector will pick up these transmitted waves of adequately fast response time and then compare them with the impinging intensity waveform. Apart from the attenuation of intensity, as with CW, this allows two more independent quantities to be extracted; a phase shift (π) and a decrease in modulation depth (ratio of AC to DC component). These variables can be changed by tissue absorption and dispersion, so that these parameters (i.e., μa, μs) can be distinguished in principle.

Time Domain FNIRS

Time Domain measurements use photon pulses of extremely short duration (100 ps or less) to irradiate the tissue and rapidly responding detectors to record the light pulse shape as it exits the tissue.

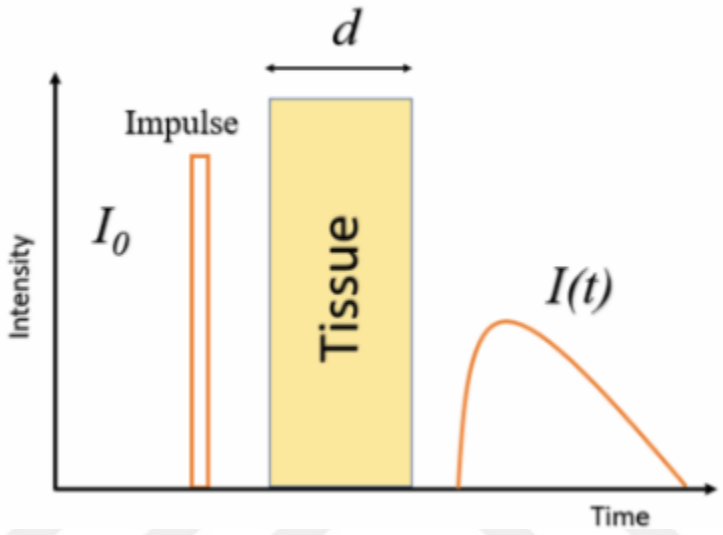

Figure 2.5. Time Domain.

Reference: Scholkmann F, Kleiser S, Metz AJ, Zimmermann R, Pavia JM, Wolf U, Wolf M. A review on continuous wave functional near-infrared spectroscopy and imaging instrumentation and methodology. Neuroimage. 2014 Jan 15;85:6-27)

Each photon's statistical encounter with a distinct amount of scattering occurrences and their variable travel paths of randomly distributed lengths lead to smearing-out overtime of the originally tightly focused impulse. The characteristics of the photon distribution received, for example, the area under the curve, the maximum time and width permitted for the evaluating the properties of tissue absorption and scattering (7).

When an external stimulus is given to the brain, an electrical signal is generated that requires oxygen and creates neuronal activity between the nerve cells. During this

process, the increased oxygen requirement is achieved, particularly by the increase of regional cerebral blood flow in the gray matter. Following this neuronal activation, there is a hemodynamic response that shows an increase in local arterial vasodilatation and a decrease in deoxyhemoglobin (HbR) and an increase in oxyhemoglobin (HbO). This mechanism is known as neurovascular coupling. NIR light is absorbed by the pigmented compounds (chromophores). The NIR light penetrates into human tissues and the NIR light scattered through the tissues. The reason for the weakening of the NIR light in the tissue at a high level is the chromophore hemoglobin (the red blood cell protein that carries oxygen, the functional group responsible for the absorption of light in the molecules). The FNIRS method offers the opportunity to learn about the oxygenation-related part of the changes especially occurring in the venous compartment. The hemoglobin absorption spectrum depends on the level of oxygenation.

With the aid of the flexible sensor used in the FNIRS systems, the recording is carried out from the different brain regions of an individual. In FNIRS, the photons that go through the brain region follow the path in the form of 'bananas' at a predictable amount. These photons can be measured by photodetectors as they are absorbed by the tissues and scattered back (16). When we examine the working principle of FNIRS; a light pattern that is scattered within the tissue is needed to measure hemoglobin concentration changes for the absorbent species. There are two analog data obtained from the textures using the wavelengths used by the FNIRS imaging method (17). These; oxyhemoglobin (HbO) and deoxyhemoglobin (Hb). Total hemoglobin (tHb) is obtained from the sum of the two. The modified Beer-Lambert law (MBLL), known as the traditional theory to calculate the change in concentration of oxy- and deoxyhemoglobin (17). This law is based on the absorption of near-infrared light by HbO and Hb. It is known that infrared light from 730nm to 850nm wavelength is used for the evaluation of brain activation by non-invasive methods. Absorption and scattering measurements at two wavelengths are calculated by varying the concentrations at which the chromophores are linked. The MBL law consists of two basic conceptual parts: 1) The extent of the path length of the light traveling to the

tissue, and 2) The extinction coefficient of the absorbent species (18). The amount of change in concentrations in the chromophores is measured using the law of the mBL. Thus, FNIRS technology is available for hemodynamic studies related to the brain. This method can be used in motor activities as well as various types of brain activity such as visual activation, auditory warning, and different cognitive task performance such as working memory, attention, visual-spatial memory and etc. FNIRS, is an appropriate imaging method in terms of both spatial and temporal resolution.

The distance between the emitter and the detector is normally kept in a specific interval because it plays a key role in measuring FNIRS. The source-detector separation of less than 1 cm could include just the input of skin layers, and the separation of more than 5 cm could lead to poor signals (20). Moreover, 3 Emitters and 8 detectors may be necessary to sufficiently obtain some prefrontal brain signals (8, 21, 22).

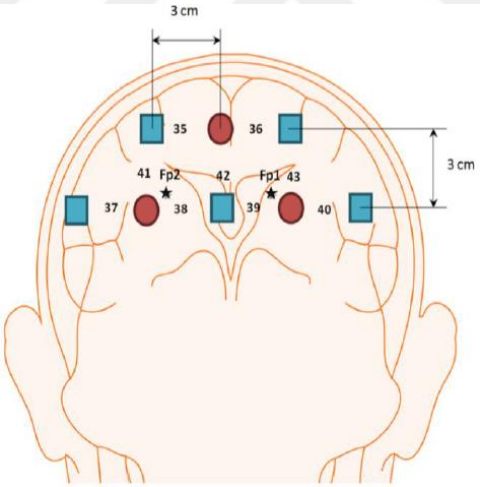

Figure 2.6. Emitter/detector pairs for Prefrontal Cortex.
Reference: Naseer N, Hong KS. FNIRS-based brain-computer interfaces: a review. Frontiers in human neuroscience. 2015 Jan 28;9:3.

2.3. Noise in FNIRS

In general, there are three different types of sources that can affect NIRS measurements. These are instrumental noise, experimental errors, and physiological noises.

Biologically hemoglobin oscillations in the bloodstream may cause the physiological noises in the measurement. In the measurements, electrical oscillations from different electronic devices can create noise for the NIRS measurement. By applying low-pass filtering, many types of high-frequency instrumental noise profiles can be removed from the physiological signals. In order to optimize signal quality in the measurement, several methods can be implemented into the measurement in terms of instrumentation. For instance, determining the laser intensity for different wavelengths, external light, and other electrical interference can affect the quality of measurement.

Three major types of noises in FNIRS signals are:

1.Instrumental noise,

2.Experimental error

3.Physiological noise

As instrumental noise and experimental error are not associated with brain activity, it is better to eliminate them before translating raw optical density signals to variations in HbO and HbR concentration (18). Instrumental noise is the interference of FNIRS signals existing in equipment or induced by the environment surrounding them (i.e. instrumental degradation is an example). Constant high frequencies are usually involved. A low-pass filter can easily remove such high frequency. In addition, instrument noise can be dramatically decreased by reducing the variability of ambient light.

Experimental noises may affect the quality of the NIRS measurements. For instance, motion artifact one of the most important issues in brain signal measurements. In functional MRI, motion artifact may happen while the subject moves in the MRI scanner. However, in optical imaging especially, NIRS measurement, the movement of optical fibers on the area that probe placed may cause the motion artifact. Moreover, in contrast to fMRI measurement, there are some NIRS applications that allow freeing movement without any restriction. Therefore, it is very significant to design the probe placement on the user.

• Experimental errors involve motion artifacts such as head movements that cause optodes from the assigned locations to be relocated. This can lead the light intensity to alter suddenly, ending up a spike-like tone.

•In the literature, below filtering methods are used commonly for motion-artifact correction:

Wiener filtering-based method (34)

Eigenvector-based spatial filtering (30)

Wavelet-analysis-based methods (21)

Savitzky-Golay type filters (35, 36)

Systemic physiological hemodynamic fluctuations such as cardiac pulsation, respiratory signals, and blood pressure changes, can occur in the superficial layers of the human brain and the NIRS measurements are much sensitive to absorption changes in these regions.

FNIRS measurements are contaminated with physiological noises that are not immediately linked to cortical brain activity that may affect Signal-to-Noise Ratio (SNR) negatively and may be similar to hemodynamic feedback in the brain. As a result of this, the result may be seen greater or less than the actual one (28). Scholkmann (7) assessed the source of these parts as well as the techniques established

to decrease the effect on the assessment of brain activity by FNIRS. Briefly, those physiological alterations add an extra quantity of variance to the FNIRS inputs.

Although there are many studies have focused on FNIRS and its noise problems, there is no main analysis technique to remove systemic physiological noise in the neuronal activity related brain hemodynamic signals. Systemic physiological fluctuations can be produced with heart rate (~1Hz), breathing rate (~0.3Hz), Mayer waves (~0.1Hz), and very low frequency (< 0.04, VLF) oscillations may cause a change in the FNIRS signal (18).

When all these procedures are approximately standardized for all other modalities of neuroimaging like fMRI, this is still not the case for FNIRS. Hocke (47), previously identified that often there is an absence of helpful data in FNIRS journals, and there is an enormous variation in the analytical procedures and description of techniques. For example, as a result of the lack of standardization pre-processing of FNIRS, the analysis may cause inadequate papers or studies and results that are not reproducible. Furthermore, the scientists showed how the use and collaboration of distinct techniques (e.g., requirements for recognizing loud transmissions, adjustment of movement artifacts, processing of waves, etc.) could contribute to distinct outcomes, affecting neuroscientific findings. A further appropriate point is the greatest FNIRS extracted sample to infer functional brain activity, as both HbO and HbR are measured by FNIRS. Several articles, for instance, take only on neuroscientific findings HbO. Others, however, report total hemoglobin (HbO+ HbR), while others define both HbO and HbR. Thus, there is an immediate need to advance towards standardizing the laboratory processes straight through to the submission of outcomes from either the study design stage.

2.4. Filtering Of Noises In The FNIRS Signal

There are some filtering methods to remove physiological noises from the FNIRS measurement which are commonly band-pass filtering, adaptive filtering, PCA, and independent component analysis (ICA). With simple low-pass, or a high-pass, or band-pass filtering, physiological noises can be removed (25). Butterworth filters are used as band-pass filtering (22). However, band-pass filtering cannot be executed to remove physiological noise whose frequencies overlap with the band of the hemodynamic response signal, respiration rate can be an example of that condition. Zhang and colleagues (32) developed the principal component spatial filter to eliminate the global systemic effects from FNIRS data. Moreover, with additional devices, for example, using PPG, the blood-related low-frequency signals in peripheral sites can be removed from prefrontal FNIRS measurement (33).

The types of techniques to remove systemic physiological noise in the neuronal activity related brain hemodynamic signals can be classified with below parameters (1):

- Signal (ΔOD or ΔHbO and ΔHbR)
- Applied Filter (e.g., Butterworth, finite impulse response (FIR), Moving Average)
- Characteristic (low-pass (LP), high-pass (HP), bandpass (BP) filtering)
- Filter Order,
- The cut-off frequencies (Fc)

Different techniques involving principal component analysis, independent component analysis, adaptive filtering, band-pass filtering, could be executed to get rid of noises. Several cognitive and motor studies showed positive results employing basic low-pass or high-pass filtering or band-pass filtering to eliminate physiological noise Different cut-off frequencies for band-pass filtering were recorded in the publications, for example:

•0.01∼0.8Hz (22)

•0.1∼0.5Hz (25)

•0.01∼0.2Hz (37)

•0.1∼0.5Hz (27)

Overall, the 0.1-0.4Hz band can potentially eliminate a large amount of physiological noise, involving heartbeat and Mayer waves, without removing the FNIRS signal generated by a 10s task.

The types of band-pass filtering include:

•Butterworth filters (13, 22)

•Elliptic filters (25)

•Chebyshev filters (38).

No clear benefit of a specific filtering approach has been documented over other methods, though. FNIRS signals are also influenced by skin blood flow and other superficial tissue interventions It has been shown that the elimination of these objects from cerebral signals can be accomplished by using various methods such as:

•The use of additional short-distance detector(s) (22),

•Statistical parametric mapping in which the artifacts are included as regressors into the model. (29)

Band-pass filtering cannot be used to filter physiological noises whose frequencies overlap with the band of the hemodynamic response signal, for example, due to respiration.

•Adaptive filtering (31, 32)

•Principle Component Analysis (30)

•Independent Component Analysis (10, 39),

However, in situations where both neural and physiological signals exist within a near band, more sophisticated methods such as adaptive filtering, independent component analysis, multi-optode layout, etc. can be used.

After optical signals have been checked and corrected for motion artifacts, there will still be several other sources of noise in the data. Physiological systemic noise arising from the cardiac cycle, respiration, systemic blood pressure, and Mayer wave fluctuations are a common component of signal interference in NIRS measurements. In fact, the absence of cardiac and other fluctuations can be a sign that data quality is low (perhaps because of poor coupling of the optical probe with the head) and often serve as a quality assurance test to indicate that functional analysis will not be possible. To remove the particular frequency band from the signal, the bandpass filter can be implemented. It can help to reduce the physiological noises from the measured signal.

2.4.1. Band-pass filtering

Different types of band-pass filters are able to remove the physiological noise in brain FNIRS measurement. In the literature, there are examples of the band-pass filter (24, 25). Furthermore, different cut-off frequencies for that filtering are also mentioned in the literature (25). For instance, have used the frequency bands of 0.01∼0.2 Hz, and 0.1∼0.5 Hz have been used in studies of Hu (25) and Tomita (27), respectively. In the case of a task of a 10 s period, the band of 0.1∼0.4 Hz can help to get rid of the major part of physiological noises such as heartbeat and Mayer waves. During the noise removal, the FNIRS signal quality can be stable. There are also different types of bandpass filtering including Butterworth filters in the literature (23). However, there is a still gap to find the absolute advantage of this filtering method.

Bandpass filtering can ensure a technique for efficiently reducing many components of noise in the data, which extracts particular frequency data from the

measured data. High-frequency instrument noise and rapid cardiac oscillations can be excluded with low-pass filters. High-pass filters that extract slow, low-frequency data can be used to extract physiological noise, such as fluctuations of blood pressure usually observed between 0.08–0.12 Hz or oscillation frequency of the heart (around 1 Hz, 60 beats/min). While bandpass filtering can be used to extract excessive low and high-frequency noise, these methods must be used cautiously to prevent the random removal of related frequencies. Bandpass filtering can therefore usually not be used to extract respiratory signals and several blood pressure signal elements, as these involve frequencies that interfere with the standard hemodynamic response data. As a consequence, bandpass filtering cannot be used to extract these particular consequences without compromising the frequencies of the stimulus-response.

2.4.2. Low&high pass filtering

Low-pass filters can also be implemented to get rid of instrumental noise in high frequency and the fast-cardiac oscillations. On the other hand, with high-pass filters, slow and low-frequency content, such as blood pressure oscillations, which are generally found between 0:08– 0:12 Hz, or cardiac pulsation (around 1 Hz, 60 × beats= min) can be removed. Even though bandpass filtering can be implemented in order to optimize signal quality, with low- and high-frequency noise, the functional hemodynamic response may be removed. Therefore, while bandpass filtering is applied, the frequency band should be chosen carefully in order not to cover the hemodynamic response. In fact, in some cases, it is hard to implement a bandpass filter since respiratory signals and blood pressure signals may overlap with the hemodynamic response.

2.4.3. ICA and PCA

Band-pass filtering cannot be efficient to eliminate physiological noise signals overlapping with the interval of the hemodynamic signals. Therefore, adaptive filters, PCA and ICA can be executed to remove physiological noise (25, 31). With PCA, the highest amount of spatial covariance among channels in FNIRS measurement can be determined and then remove those parts from all channels. As a result of this, the output can weight more towards neurovascular coupling than systemic physiology (40, 41).

Independent component analysis (ICA) method can eliminate physiological noises from hemodynamic response signals. With the spectral densities of the physiological signals, independent components (IC) can be determined. The main IC associated with the hemodynamic response signals can be separated and the obtained signals can be physiological noise-free (26).

Moreover, PCA can be used to remove systemic physiological noise in the neuronal activity related to brain hemodynamic signals. Its method is similar to the motion artifact removal process since systematic fluctuations are covariant in the different channels of FNIRS measurement. (13). There are some parameters that may affect the efficiency of PCA, for example, the number of channels and the number of eigenvectors to be removed (42). Therefore, if there is a low number of channels, different methods can be executed instead of the PCA method. Like the bandpass filter, a real-time solution of ICA for physiological noise removal is still not a gold standard.

PCA utilizes a linear orthogonal transformation method to transform the time-course of the signal between all N channels into an uncorrelated collection of N factors. The eigenvalues and eigenvalues vectors are obtained from the measurement covariance matrix. Since the movements make up the bulk of the signal variety, it is presumed that the bigger own values indicate the variance induced by movement

artifacts. Thus, by removing the first k's own values, a particular proportion of the signal variance will be removed. (42)

2.4.4. Correlation-based signal improvement (CBSI)

The correlation-based signal improvement (CBSI) is a channel-by-channel solution established to reduce motion artifacts induced by the head movement. (5)

The CBSI technique is based on the theory that HbO and HbR are negatively correlated and are only strongly linked when a movement artifact happens. This technique is therefore based on two hypotheses: (1) the real HbO and HbR (x0 and y0) should be negatively correlated (x0*1⁄4 −βy0) and (2) the correlation between the real HbO and the movement artifact (F) should be near 0. The HbO and HbR (x and y) assessed are modeled as follows:

$$x = x_o + \frac{std(x)}{std(y)} * F + Noise \quad y = y_o + F + \text{Noise} \qquad \text{(Eqn 2.2.)}$$

Where std is the standard signal deviation. Then the following corrected signal can be achieved by applying the two previously mentioned assumptions to the model and considering α 1⁄4 β:

$$x_o = \frac{1}{2}\left(x - \frac{std(x)}{std(y)} * y\right), \; y_o = \frac{std(y)}{std(x)} * x_o \qquad \text{(Eqn 2.3.)}$$

Please notice that the "x0" and "y0" corrected signals are not HbO and HbR and are merely a linear combination of measured HbO and HbR signals.

Unlike PET and fMRI, there are no gold standard methods for FNIRS data analysis. So far, some methods of analysis have been shown and tried to be proved. This situation may not cause a problem, since, it may be helpful to execute non-standard analyses of NIRS data. Creating the most suitable method for FNIRS data analysis always becomes a problem for new beginners FNIRS users. It takes time to implement analysis such as multi-channel FNIRS data. Therefore, there may be

essential to create a toolset for preprocessing analysis. Generally, those methods based on fMRI data analysis.

Statistical parametric mapping (SPM) relates to the building of statistical procedures that are spatially expanded to check hypotheses of regional particular impacts. SPMs are imaging process with voxel characteristics which have a recognized distributional (generally Gaussian) estimate under the null hypothesis. The strength of statistical parametric mapping is mainly attributed to the ease of the fundamental concept: namely one uses any (univariate) statistical parametric sample to analyze each voxel.

Statistical evaluation of task-evoked hemodynamics

The general linear model (GLM) is commonly executed in fMRI (35) and FNIRS (36) studies as a statistical technique for modeling task-related activation. The GLM makes the task activation to be calculated by describing the time series reported as the linear composition of several sources, namely the predicted hemodynamic response plus a set of error terms (35). GLM is used to analyze differences between groups or circumstances as it is easier to apply using multi-level analysis(28) and the variance between subjects is standardized, leaving large group differences.

Nevertheless, considerable variation in the form and timing of the hemodynamic response of a subject at the level limits the accuracy of simulation activation with general linear regression (37). It was agreed in the fMRI literature that using hemodynamic-based alternatives could boost GLM calculations by taking into account individual differences in hemodynamic response (38,39), yet the FNIRS group has only recently acquired the concept. Faced with this concept of enhancing precision by collecting individual differences in hemodynamic response, a new advanced approach by Pinti et al. (40) tries to do just that by automatically detecting the different evoked

hemodynamic shapes and features. More research is needed to assess the sensitivity and specificity of this approach to specific changes that have been evoked. More scientific research into new automated methods for detecting brain activity in real-world situations, like the one developed by Pinti et al.(40), will speed up new FNIRS imaging applications.

Meanwhile, researchers from beginner FNIRS must remain carefully aware of how computational processing steps can function to change their performance. This paper provides a simple view of the effects of specific preprocessing phases while examining standard de-noising methods with regard to their influence on the sensitivity and specificity of hemodynamic activation with general linear modeling, with and without derivatives.

3. MATERIALS AND METHODS

PubMed database and a manual search from articles, references, and the publication surveys made available by the Society for functional Near Infrared Spectroscopy (http://FNIRS.org/publications/nirs-niri-publications/) were used to find common filtering models to eliminate the systemic physiological noise in the neuronal activity related brain hemodynamic signals. During the research, we concentrated on techniques on concentration changes of oxy- and deoxyhemoglobin. Since continuous wave (CW) FNIRS in current FNIRS research and neuroscience applications are more common.

With careful planning, all the filter types had been according to the definition of the experimental tasks, developing the contrasts, and selecting the times of repetition and duration. To subtract "false" hemodynamic / oxygenation reactions from the test assignment, the functional procedure must have the highest feasible basis situation.

3.1. Experimental Protocol

3.1.1. Participants

According to clinical and radiological criteria, fifteen subject (12 females/3 males) who were diagnosed as knee osteoarthritis patient and had chronic pain in the right or left knee. The subjects were recruited from Haydarpaşa Numune Training and Research Hospital Clinic of Orthopaedics and Traumatology.

Spontaneous changes in prefrontal cortex hemodynamics were measured using the functional near-infrared spectroscopy measurements were performed with a continuous wave multi-channel NIRSCout device at the beginning of and within one

week after the treatment (NIRX Medical Technologies LLC, Berlin, Germany). NIRSStar software was used for data recording (NIRx Medical Technologies LLC, Glen Head, NY, USA). The signal sampling rate was 4.17 Hz. 15 detectors and 15 sources which form a 47 channel setup with an inter-probe distance of a maximum of 3 cm was used. According to the subject's head circumference (56 cm and 58 cm), EEG cap (EASYCAP, Herrsching, Germany) sizes were determined. Channels and their locations in the different brain regions are demonstrated in Figure 3.1 and described below:

- DLPFC=[1 2 3 4 9 11 19 20 21 23 6 17 27 38];
- PMC=[45 46 29 24 40 26 37 35 34];
- PSMC=[12 28 41 39 30];
- FP=[7 8 10 13 14 15 16 18 5 22];
- SMC=[31 32 33 42 43 47 36 25 44];

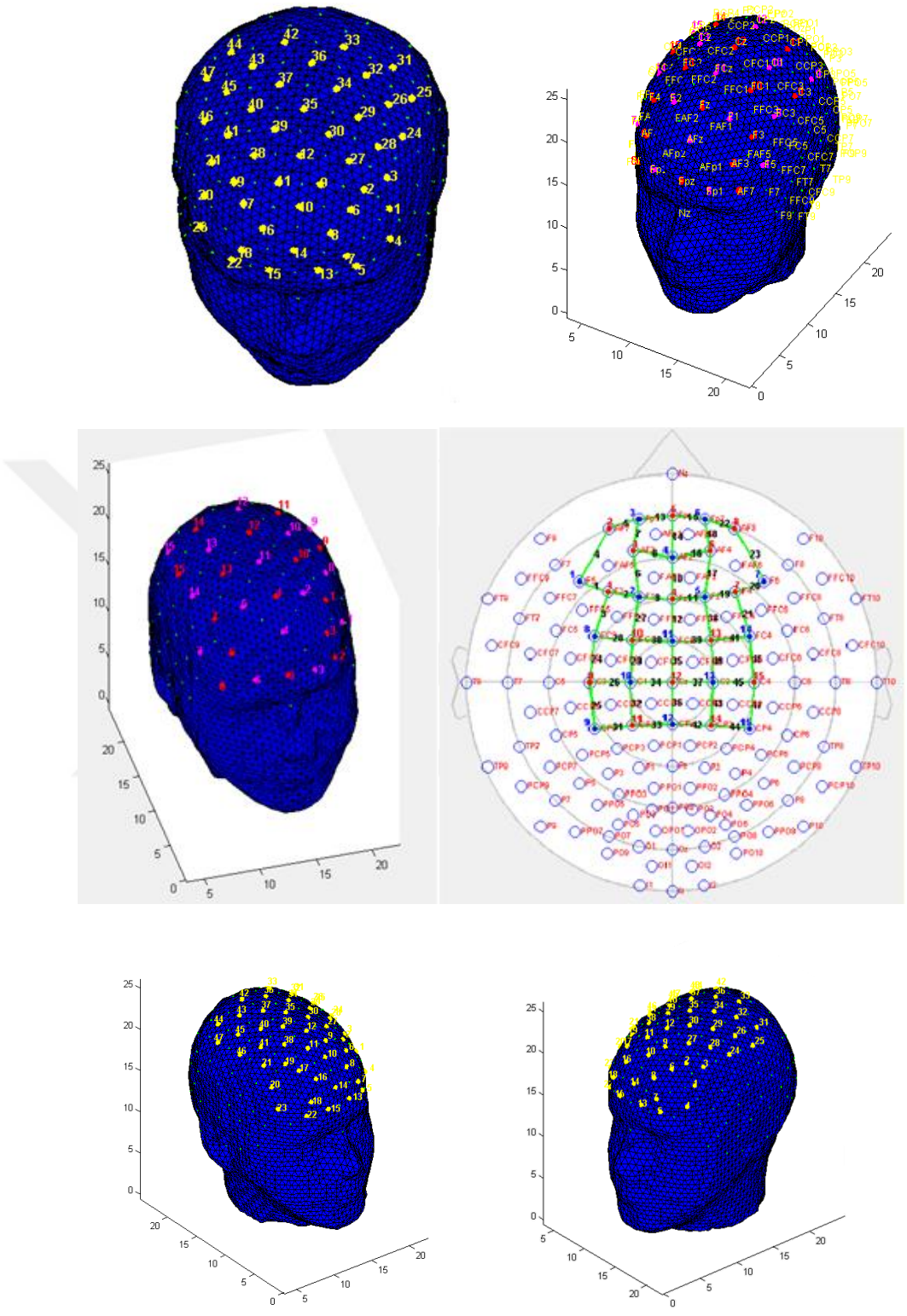

Figure 3.1. Probe configuration and channel set-up.

3.1.2. Experimental design

Subjects sat on a chair and the computer system was located 1 meter away from the subject. The screen which was placed about 1 m away from the eyes during the experiments. Subjects kept their eyes open and not move their heads. With a digital algometer (Wagner Force Ten FDX 50 Wagner Instruments, Greenwich, CT), the level of painful stimulation was determined. The applied stimuli locations were from i) 3 cm medial to the medial edge of the patella and ii) 3 cm inferior to the inferior edge of the patella (46). Using the Verbal Rating Scale, subjects determined their pain level with a score out of 10 points at the end of each task. Painful stimuli were graded with each subject's score. Subjective scales above 5 points were decided as painful stimuli and this value was recorded. 5 N was considered as a non-painful stimulus. The recorded pressure threshold values were used in the actual FNIRS experiment. During the experiment, the operator used the probe before the experiment so that the pressure and the pressure increase rate were kept stable. Pressure was measured in Newtons (N).

The experimental protocol took 20 minutes. The experiment began with a 60 second of baseline measurement. NIRSStim program was used for arranging the stimulus timing. Painful (P) and non-painful (NP) stimulations were presented randomly and each was applied 15 times. The stimulus duration was 5 seconds with a 30 second inter stimulus interval (ISI).

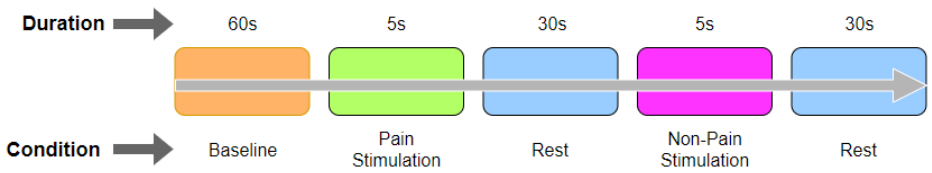

Figure 3.2. Experimental procedure.

3.1.3. FNIRS Data Acquisition

Since FNIRS is one of the most recent neuroimaging modalities, there is no consensus on a standardized way of analyzing data and setting the methodological details in research articles. Depending on the filter types, the filters would be applied to optical density data or concentration data. For the statistical analysis, the Homer2 software package was used to apply different filter types with different characteristics given as options.

The HomER software is based on an adaptable data design that enables the import of data from practically any current commercial NIRS system with limited preparatory processing. Evaluation of this information can be customized to allow users to define the information of their study, including geometry and configuration of the NIRS probe, optical wavelength choice, stimulation layout, as well as other variables of instrumentation and data acquisition.

The HomER program has been produced and is accessible at the Massachusetts General Hospital's Photon Migration Imaging Laboratory. This program is provided as open-source software as well as a written standalone executable binary program in its indigenous MATLAB format (18). The main aim of the HomER software design is to ensure users with simple, fast, and efficient information communication and simulation. The software was designed to enable the user to interact with their information from the point of an overview, the positioning of large amounts of data, to the comprehensive management of individual time tracks from a single measurement between a source and detector pair (18).

As the NIRS concept keeps progressing, the growth of standardized processing and assessment instruments is becoming increasingly necessary. In the context of discussing these techniques, the applicability of these techniques in HomER is defined as a program for functional NIRS data analysis and visualization. (18).

HomER, an expression for the optically evaluated hemodynamic evoked response, is a set of open-source MATLAB (MathWorks, Natick, Massachusetts) applications that are interfaced by a front end graphical user interface. The HomER software enables the user to compute hemodynamic alterations in levels of oxyhemoglobin and deoxyhemoglobin from time series of raw light intensity obtained at various wavelengths for fundamental assessment. The system includes a variety of signal processing instruments for further sophisticated assessment, such as bandpass filters for removing instrumental or physiological noise contributions, subject movement correction filters, and principal component-based filters to remove systemic physiology (19).

HomER already includes multiple techniques for block averaging and linear regression of stimulus periods as blocked, event-related, and multiple condition experimental designs for traditional analysis of functional data. With comparative statistical analysis, it is possible to determine both single subject and group-averaged reactions.

3.2. FNIRS Data Analysis

3.2.1. Preprocessing pipeline steps and options

3.2.1.1. Channel exclusion criteria

A variety of factors can degrade signal quality, involving instrument and environmental noise, the weak coupling of optodes to the head, artifacts caused by motion and optical interference by heavily pigmented hair (6). These sources of interference and artifact may lead to lower signal-to-noise ratio (SNR), sharp spikes in the datasets, and/or rapid changes in baseline frequency, resulting in incorrect measurement and misinterpretation (7,8). It is important to establish a standard to exclude weak channels that would otherwise reduce the quality of data in order to ensure sufficient signal quality.

A commonly used test is the visual inspection of the optical density signal of ~830–850 nm wavelength in the time or frequency domain for the presence of cardiac pulsation. The theory is that the existence of a strong and stable cardiac oscillation suggests that shifts in optical density are associated with hemodynamic physiological alterations. Nevertheless, the visual inspection approach has some disadvantages, i.e. (1) this does not provide that the ~700 nm wavelength signal is of enough quality (this wavelength is assigned to deoxyhemoglobin and therefore cardiac pulsation is less stable), (2) it is qualitative (highly evaluator-dependent), and (3) it is time-consuming, making it ineffective for large datasets. For such purposes, automated channel exclusion approaches would be beneficial as far as they are working on a level with or greater than visual inspection. Many computational automated techniques for analyzing and defining mechanisms for channel exclusion have been investigated in the literature.The two automated criteria we will investigate are the widely used coefficient of variation (CV) method and the method developed by HOMER.

The two computational automated parameters that will be examined in this study are the commonly used method of variation coefficient (CV) and the 'enprunechannel' method has developed in HOMER2.

enPruneChannels function from Homer2 was applied to exclude the noisy channels. According to the large standard deviation interval, too weak or too strong signals, channels can be pruned by this function. We used this function with the 2% SNR threshold. As a result, all channels passed the thresholds defined by the enprunechannels function.

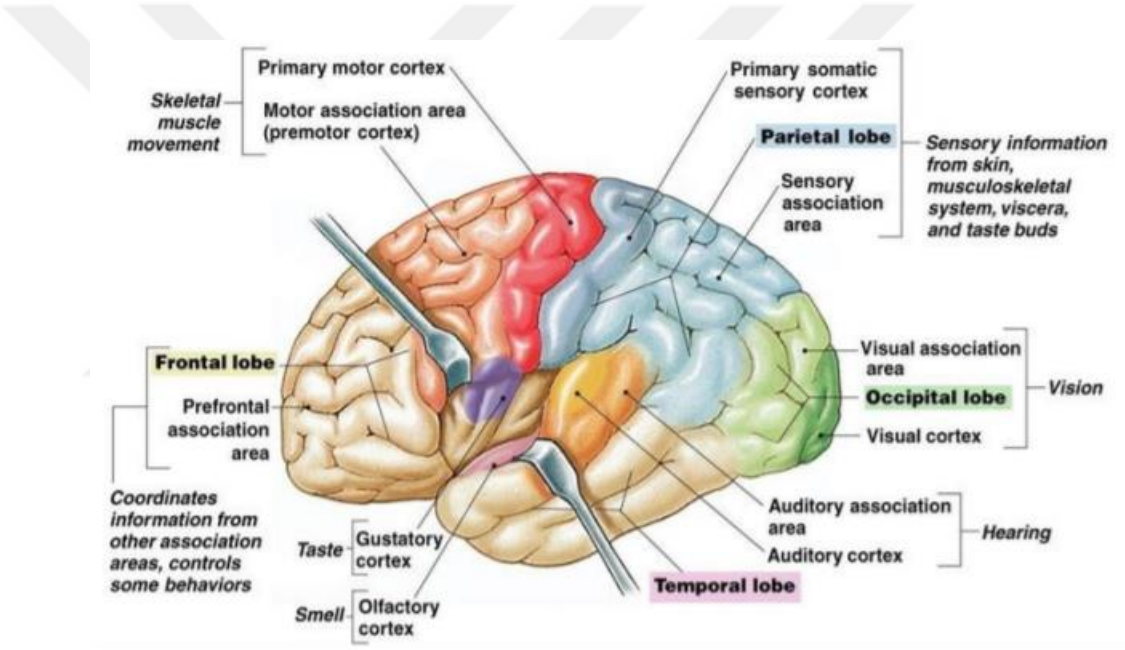

Figure 3.3. Brain regions with associated tasks.
Reference: Sato T, Nambu I, Takeda K, Aihara T, Yamashita O, Isogaya Y, Inoue Y, Otaka Y, Wada Y, Kawato M, Sato MA. Reduction of global interference of scalp-hemodynamics in functional near-infrared spectroscopy using short distance probes. NeuroImage. 2016 Nov 1;141:120-32.

3.2.1.2.Motion correction

Identifying and eliminating signal artifacts caused by motion of the subject is also significant. In general, motion artifacts are characterized by quick alterations in intensity that are greater than the alterations in hemodynamics. It is significant to remember that algorithms for eliminating the motion artifacts are very useful

techniques that, if used in the not correct way, can reduce the quality of the output signals. Some of these methods have multiple variable variables and may not be ideal for all datasets with the defaults. Also, the advanced methods listed here, can introduce spurious artifacts if they are used with the wrong criteria,

With the hmrIntensity2OD function from Homer2, the intensity data were converted into changes in optical density. To identify the motion artifact in the channels, the hmrMotionArtifactByChannel function was used with a defined standard deviation threshold and amplitude threshold of the signal. If there is any motion artifact, the data segment around that time point is marked. It has been set out without causing a change in the experimental design. Then, as a result of this, denoising methods can be implemented effectively.

In the present study, three motion correction approaches which are among the most commonly used methods in FNIRS literature were selected for comparison. These were correlation based signal improvement method (CBSI), principal component analysis (PCA) method and the spline interpolation method. (5)

CBSI technique relies on the assumption that if the data is exempt from artifacts, time series of HbO and HbR should always have a negative correlation. Head motion-induced noise during the experiment is expected to cause a positive correlation in the signal since a motion artifact would cause the same directional change in the HbO and HbR time series. CBSI can correct for motion artifacts by identifying regions where the anticorrelation is violated. With the CBSI method, the spikes in the signal caused by motion can be removed. Even, it can be implemented to the condition with minimal noises. For the CBSI technique, the OD values are needed to be converted into the HBO and HBR concentration data. Hence; the concentration values were first obtained with hmrOD2Conc function.

Principal component analysis

Principal Component Analysis (PCA) is a computational technique that uses an orthogonal transformation to translate a dataset of potentially correlated variables (entities each assuming different numerical values) into a dataset of linearly uncorrelated variables called principal components. This conversion is described in such a way that the first major component has the greatest possible variance (i.e. accounts for as much variation as possible in the data), and each successor component, in turn, has the highest possible variance under the constraint that it is orthogonal to the preceding components. The resulting vectors (each being a linear combination of the variables and containing n observations) are an uncorrelated orthogonal basis set. PCA is sensitive to the relative scaling of the original variables.

PCA's algorithm converts a NIRS dataset with N time points into linearly uncorrelated N elements, ordered by their correlation to data variance. Normally, the amplitude of motion objects is much greater than the NIRS signal in the field. Usually, there are also motion artifacts on several NIRS channels. The approach of PCA to the processing of NIRS data is based on the fact that motion artifacts provide the superior contribution to the variance of the NIRS data and that the first r theoretical components will therefore only compensate for motion artifacts. These r components can then be removed prior to further analysis. For a NIRS dataset Y, of dimensions time × channel, the PCA motion correction consists of first performing a singular value decomposition on the spatial correlation matrix YTY such that:

$$YTY=U\Omega UT \quad \text{(Eqn 3.1.)}$$

Where U is the orthogonal matrix of spatial eigenvectors and Ω is a diagonal matrix of the associated eigenvalues, both of dimensions N × N (Zhang et al., 2005). The first r eigenvectors can then be removed from the data, such that:

$$Ycorrected=Y(I-UArUT) \quad \text{(Eqn 3.2.)}$$

Where Ar is an N × N matrix with the first r diagonal elements equal to 1, and all other elements equal to zero. The performance of PCA in removing motion artifacts from NIRS data is heavily dependent on two factors: the number of NIRS measurements in a dataset [as this defines the number of components (N)] and the number of components that are removed (r). A simple way to approach the selection of r is to normalize the diagonal elements of the matrix Ω by their sum to produce the vector Ω˜. The nth element of Ω˜ then provides a measure of the proportion of the NIRS data variance that is accounted for by the nth component. By fixing the proportion of data variance that is to be removed (referred to from herein as σ_PCA), the number of components to remove (r) can be defined by finding the lowest value of r for which:

$$\sum_{n=1}^{r} \Omega\tilde{}n \geq \sigma_{PCA} \qquad \text{(Eqn 3.3.)}$$

Spline interpolation

When motion artifact phases have been identified (in this case using HOMER2's hmrMotionArtifact), each of these phases is modeled one by one, using the MATLAB™ cubic spline interpolation function csaps throughout each NIRS time-course. Each modeled data phase is removed from the original data phase. To generate a continuous signal, all the data points after a constant value has changed after the start of the corrected motion section.

This value is specified as the difference between the signal mean at the beginning of the corrected motion phase and the signal mean before the corrected motion phase. The phase of the measurement of these means must be variable, since the length of the motion artifacts and the length of the data before each motion artifact is also variable. Such durations have been described using the method.

The spline interpolation depends on the interpolation parameter p_Spline. This parameter is defined in MATLAB™ such that if p_Spline = 0, the motion artifact is modeled with a least-squares straight-line fit. If p_Spline = 1, the motion artifact is modeled via a natural cubic spline interpolation. Therefore, performing motion correction with p_Spline = 0 will remove only a straight-line fit from the artifact while a p_Spline = 1 model will approximate the artifact very accurately and on subtraction leave a near-constant value. It was defined their parameter as (1−p_Spline) and suggest that a value corresponding to p_Spline = 0.99 is reliably effective in the removal of motion artifacts.

3.2.1.3.Bandpass Filtering

FNIRS measurements contain systemic physiological artifacts which stem from both systemic cerebral and systemic extracerebral (skin, bone, and cerebrospinal fluid) physiology (19). The neuronally induced hemodynamic responses in FNIRS data is known to exist in the low frequency portion of the signal, roughly within the 0.01-0.2 Hz range. Bandpass filters are commonly used to eliminate high-frequency (≥0.2 Hz; breathing, respiratory rate, instrument noise) and very low (< 0.01 Hz) signal frequency effects in the data (18).

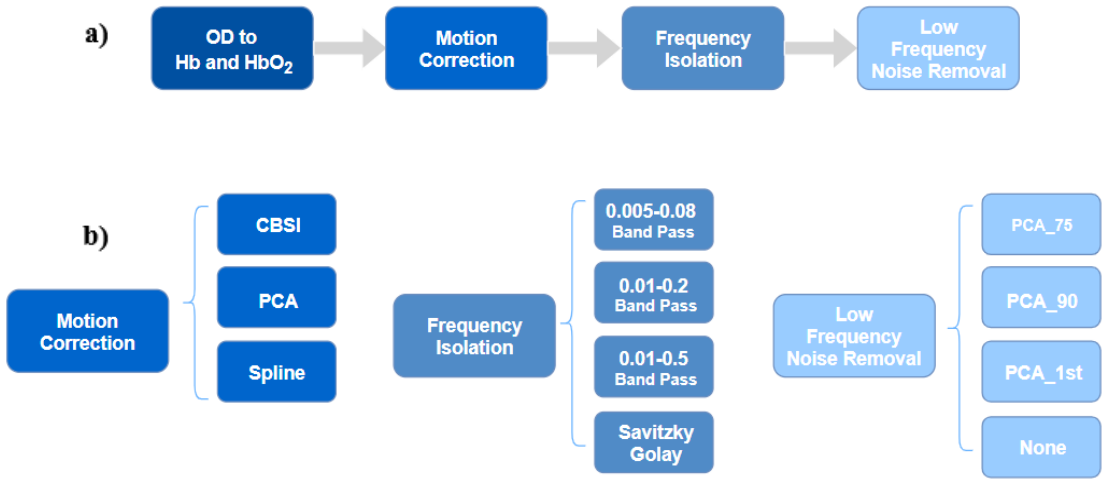

Figure 3.4. Flow diagram for different preprocessing steps and the methods tested for each step. a) The main preprocessing steps are shown. b) Different methods applied in each step are shown. The raw optical density values were first converted into concentration values. Then, in the first filtering step, CBSI, PCA and Spline interpolation methods were implemented separately. In the second step, a Butterworth filter with three different bands and a Savitzky Golay filter were applied separately to data obtained from the first step. At the end of the second step, 12 different processing options were obtained. In the third step, three different PCA based techniques and a 'None' option were applied as a fourth method on the data acquired from the previous step. In the end, 48 different pipelines were obtained.

0.01-0.2 Hz, 0.005-0.08 Hz, 0.01-0.5 Hz were determined to be the most commonly used frequency ranges and were implemented separately in order to remove physiological noises which cover heartbeat (1~1.5Hz), respiration (0.2~0.5Hz), Mayer waves (~0.1Hz) (41).

3.2.1.4. Low Frequency Noise Removal

In the last step, a different type of PCA technique was applied. Similar to the motion artifact correction version, PCA can also be used to remove low frequency noise whose frequencies overlap with the frequencies of the neuronal activity related signals, due to the assumption that systematic fluctuations will be covariant among FNIRS measurements from different channels. Decreasing covariance of the data can there fore eliminate low-frequency physiological noises from the data (13).

Application of PCA after band pass filtering ensures that common systemic global effects in the low frequency range are targeted, not the mixture of systemic effects at irrelevant frequencies (i.e., cardiac and respiratory effects) whose temporal dynamics are much different than the slowly varying neuronally induced signals.

We applied PCA with 3 options: 1) removal of 90 % of the variance (PCA90), 2) removal of 75 % of the variance (PCA75), 3) regressing out the 1st principal component (PCA1st) from each time series. We compared the impact of low frequency denoising to the case where no denoising method was applied (None).

Different Methods Used For Comparative Analysis				
Number	Method	Options		
		Motion Correction	Bandpass filtering	LF Noise Removal
1	HBO__PCA_SGfilt.mat'	PCA	Savitzky Golay	None
2	HBO__PCA_band1.mat'	PCA	0.005Hz -0.08 Hz	None
3	HBO__PCA_band2.mat'	PCA	0.01Hz- 0.2 Hz	None
4	HBO__PCA_band3.mat'	PCA	0.01Hz-0.5 Hz	None
5	HBO__SPLINE_SGfilt.mat'	Spline	Savitzky Golay	None
6	HBO__Spline_band1.mat'	Spline	0.005Hz -0.08 Hz	None
7	HBO__Spline_band2.mat'	Spline	0.01Hz- 0.2 Hz	None
8	HBO__Spline_band3.mat'	Spline	0.01Hz-0.5 Hz	None
9	HBO__band1_cbsi.mat'	CBSI	0.005Hz -0.08 Hz	None
10	HBO__band2_cbsi.mat'	CBSI	0.01Hz- 0.2 Hz	None
11	HBO__band3_cbsi.mat'	CBSI	0.01Hz-0.5 Hz	None
12	HBO__sgfilt_cbsi.mat'	CBSI	Savitzky Golay	None
13	PCA75_SGband_cbsi_HBO.mat'	CBSI	Savitzky Golay	PCA with % 75 variance removal
14	PCA75_SGfilt_PCA.mat'	PCA	Savitzky Golay	PCA with % 75 variance removal
15	PCA75_SGfilt_Spline.mat'	Spline	Savitzky Golay	PCA with % 75 variance removal
16	PCA75_band1_PCA.mat'	PCA	0.005Hz -0.08 Hz	PCA with % 75 variance removal
17	PCA75_band1_Spline.mat'	Spline	0.005Hz -0.08 Hz	PCA with % 75 variance removal
18	PCA75_band1_cbsi.mat'	CBSI	0.005Hz -0.08 Hz	PCA with % 75 variance removal
19	PCA75_band2_PCA.mat'	PCA	0.01Hz- 0.2 Hz	PCA with % 75 variance removal
20	PCA75_band2_Spline.mat'	Spline	0.01Hz- 0.2 Hz	PCA with % 75 variance removal
21	PCA75_band2_cbsi_HBO.mat'	CBSI	0.01Hz- 0.2 Hz	PCA with % 75 variance removal
22	PCA75_band3_PCA.mat'	PCA	0.01Hz-0.5 Hz	PCA with % 75 variance removal
23	PCA75_band3_Spline.mat'	Spline	0.01Hz-0.5 Hz	PCA with % 75 variance removal
24	PCA75_band3_cbsi_HBO.mat'	CBSI	0.01Hz-0.5 Hz	PCA with % 75 variance removal
25	PCA90_SGband_cbsi_HBO.mat'	CBSI	Savitzky Golay	PCA with % 90 variance removal
26	PCA90_SGfilt_PCA.mat'	PCA	Savitzky Golay	PCA with % 90 variance removal
27	PCA90_SGfilt_Spline.mat'	Spline	Savitzky Golay	PCA with % 90 variance removal
28	PCA90_band1_PCA.mat'	PCA	0.005Hz -0.08 Hz	PCA with % 90 variance removal
29	PCA90_band1_Spline.mat'	Spline	0.005Hz -0.08 Hz	PCA with % 90 variance removal
30	PCA90_band1_cbsi.mat'	CBSI	0.005Hz -0.08 Hz	PCA with % 90 variance removal
31	PCA90_band2_PCA.mat'	PCA	0.01Hz- 0.2 Hz	PCA with % 90 variance removal
32	PCA90_band2_Spline.mat'	Spline	0.01Hz- 0.2 Hz	PCA with % 90 variance removal
33	PCA90_band2_cbsi_HBO.mat'	CBSI	0.01Hz- 0.2 Hz	PCA with % 90 variance removal
34	PCA90_band3_PCA.mat'	PCA	0.01Hz-0.5 Hz	PCA with % 90 variance removal
35	PCA90_band3_Spline.mat'	Spline	0.01Hz-0.5 Hz	PCA with % 90 variance removal
36	PCA90_band3_cbsi_HBO.mat'	CBSI	0.01Hz-0.5 Hz	PCA with % 90 variance removal
37	PCA_1st_SGband_cbsi_HBO.mat'	CBSI	Savitzky Golay	PCA with first regressor variance removal
38	PCA_1st_SGfilt_PCA.mat'	PCA	Savitzky Golay	PCA with first regressor variance removal
39	PCA_1st_SGfilt_Spline.mat'	Spline	Savitzky Golay	PCA with first regressor variance removal
40	PCA_1st_band1_PCA.mat'	PCA	0.005Hz -0.08 Hz	PCA with first regressor variance removal
41	PCA_1st_band1_Spline.mat'	Spline	0.005Hz -0.08 Hz	PCA with first regressor variance removal
42	PCA_1st_band1_cbsi.mat'	CBSI	0.005Hz -0.08 Hz	PCA with first regressor variance removal
43	PCA_1st_band2_PCA.mat'	PCA	0.01Hz- 0.2 Hz	PCA with first regressor variance removal
44	PCA_1st_band2_Spline.mat'	Spline	0.01Hz- 0.2 Hz	PCA with first regressor variance removal
45	PCA_1st_band2_cbsi_HBO.mat'	CBSI	0.01Hz- 0.2 Hz	PCA with first regressor variance removal
46	PCA_1st_band3_PCA.mat'	PCA	0.01Hz-0.5 Hz	PCA with first regressor variance removal
47	PCA_1st_band3_Spline.mat'	Spline	0.01Hz-0.5 Hz	PCA with first regressor variance removal
48	PCA_1st_band3_cbsi_HBO.mat'	CBSI	0.01Hz-0.5 Hz	PCA with first regressor variance removal

Figure 3.5. Different methods used for comparative analysis.

All 48 pipeline algorithms are shown in the above table. The effects of each pipeline will be shown in the result section.

3.2.2. Performance evaluation

Data pertaining to each stimulus type were truncated 5 s before and 25 seconds after the onset and end of stimulus duration respectively. These data segments belonging to each trial were block averaged over all stimuli and metrics describing signal quality were extracted for comparison. The blocks were arranged for both pain

and non-pain tasks, covering 5s before the task and 25 s after the task. With the results obtained, the effect of each pipeline can be quantified as declared in the results section.

The block averaged signals from each preprocessing pipeline need to be compared with the ideal hemodynamic response. Therefore, with the following step, an ideal hemodynamic response (HRF) whose duration matched the defined block average duration were synthesized. Then, several performance metrics were determined. These performance metrics include correlation (R) with the synthetic HRF model, mean squared error between the HRF model and the truncated block averaged datasets, a contrast to noise ratio metric which is defined as i) difference between maximum of the signal during stimulus and mean of prestimulus baseline divided by the standard deviation of the prestimulus baseline (CNR) and as ii) maximum of the signal during stimulus divided by the standard deviation of the prestimulus baseline (CNR2), signal to noise ratio (SNR) defined as the mean of the signal over standard deviation of the prestimulus baseline, Cohen's d defined as i) the difference of the mean of the signal during stimulus and a prestimulus baseline duration of 3 seconds (COHD), and as i) the difference of the mean of the signal during 5 seconds after stimulus and a prestimulus baseline duration of 3 seconds (COHD2), Trial to trial variability (T2T) which describes the mean standard deviation among different trials of the same task, Beta weights for the canonical HRF function which is obtained by fitting a generalized linear model to the data where the canonical HRF models the signal of interes, t scores obtained from the GLM where the contrast is defined for pain, nonpain and difference conditions (T) and a custom derived metric PAR which describes the difference between the mean data around the maximum point and the mean data over the baseline period. In the next step, each parameter was normalized among 48 methods (plotting values between 0 and 1) for each channel and subject. And then normalized performance metrics for 11 parameters were calculated. By normalizing all performance metrics and merging them into a single parameter with equal weights given to each, all pipelines could be compared in terms of isolating the desired stimulus induced hemodynamic signal. One tailed, paired t-tests and the resulting statistical scores were utilized to locate the most active channels which could provide the contrast between brain activation during pain and nonpain conditions (Pain>Nonpain) for all parameters. After obtaining those active channels, the best and worst performer

methods were determined by focusing on the data of one of those channels (channel 14).

4. RESULTS AND DISCUSSION

Motion Artifact Removal

Baseline shifts, high spikes and slow-motion related drifts which are the three main causes of motion artifact, were observed in various channels. Application of each motion artifact removal technique accounted for different problems in the data and resulted in different signal waveforms. The effects of the 3 approaches were visually examined on sample channels from representative subjects. The impact of each method can be visually inspected in the below figure.

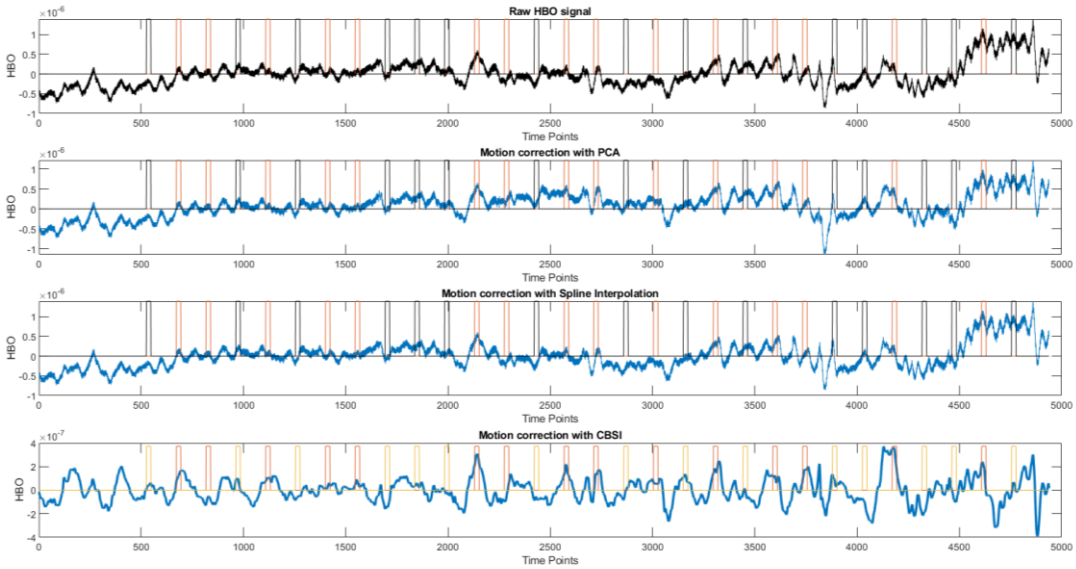

Figure 4.1. Effects of different motion correction techniques on raw HbO signal of Subject 1 channel 10.

Figure 4.2 demonstrated HBO data from another representative channel (Ch.14) from the same subject. When visually inspected, the CBSI technique performs baseline shift correction and spike removal to a decent extent as can be seen in Figure 4.2.

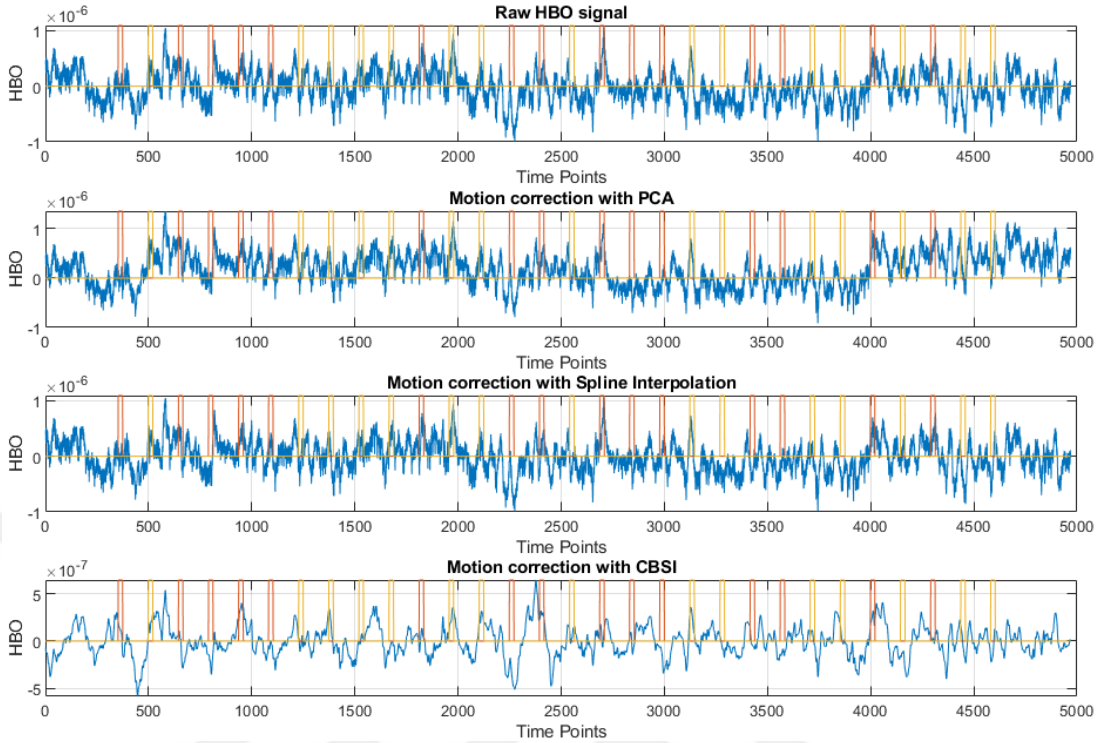

Figure 4.2. Effects of different motion correction techniques on raw HbO signal. Data is from Subject 1, Channel 14.

Band-pass filtering for Removal of Systemic Physiology

For each dataset preprocessed with different motion correction techniques, the next step is to remove the physiological and low-frequency noise effects and observe the impact of different cut-off frequencies commonly used in FNIRS literature. For this purpose, each data set was bandpass filtered with a 4th order Butterworth filter with 3 cut-off frequencyoptions: 1) 0.005-0.08 Hz, 2) 0.01-0.2 Hz and 3) 0.01-0.5 Hz. In addition to Butterworth filters, the impact of Savitzky Golay filtering with a Hanning window of 4 and 80 seconds was also examined. Hence at the end of Step 2, 4 filtering options per each motion correction technique resulted in 12 pipeline options Figure 4.3 demonstrates the impact of different filters on a representative time series data corrected with Spline Interpolation method.

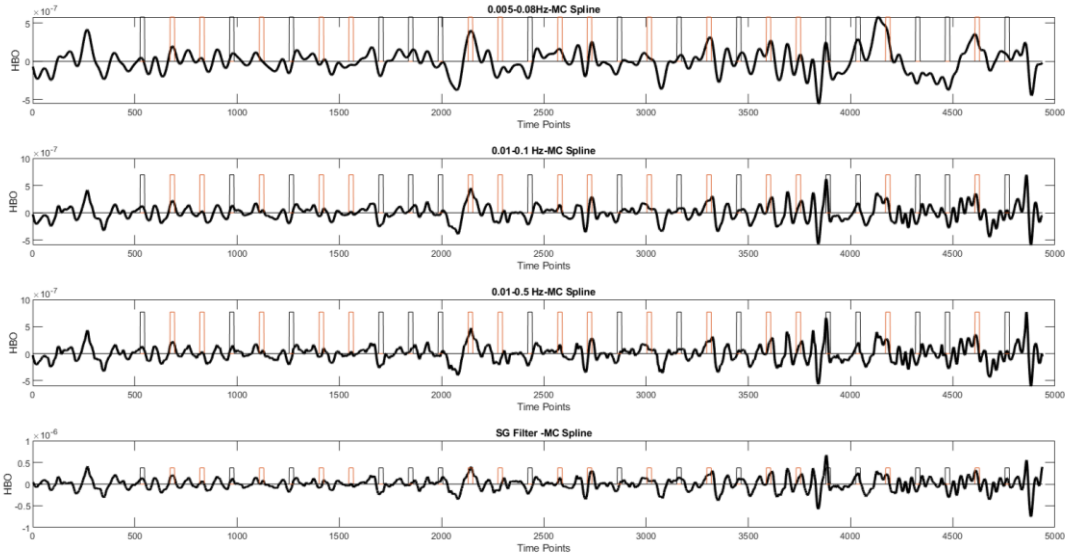

Figure 4.3. Visualization of the impact of different cut-off frequencies on data corrected with Spline Interpolation (Subject 1, ch 10 data).

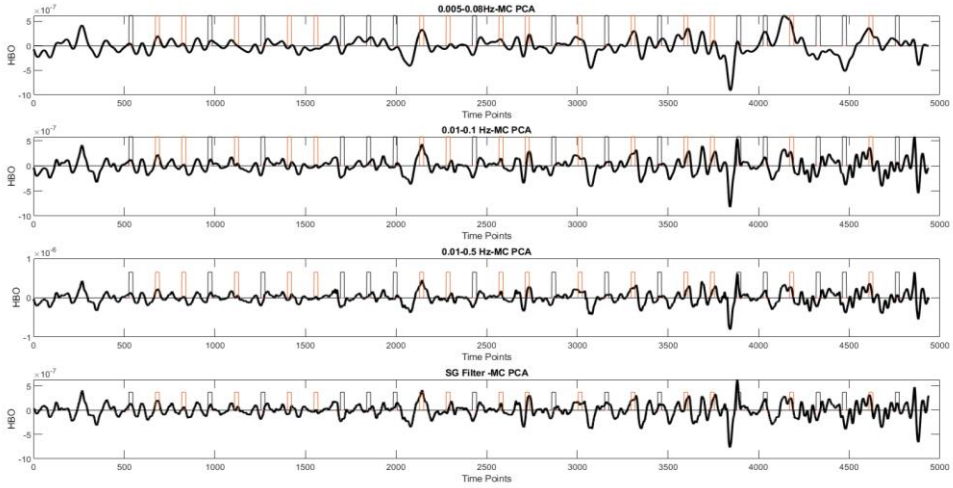

Figure 4.4. Visualization of the impact of different cut-off frequencies on data corrected with PCA (Subject 1, Ch 10).

Similarly, the impact of different filters on a representative time series data after correction with PCA and CBSI methods can be visualized in Fig.s 4.4. and 4.5. respectively.

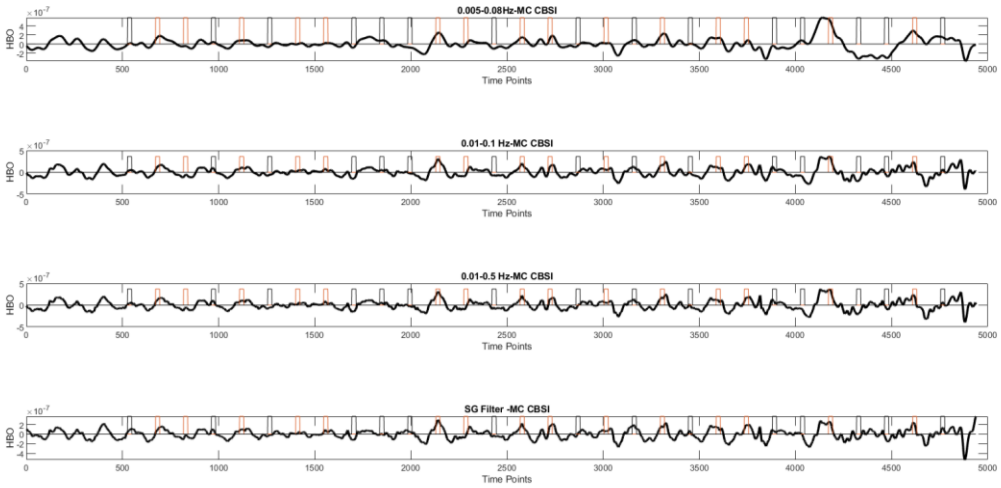

Figure 4.5. Visualization of the impact of different cut-off frequencies on data corrected with CBSI (Subject 1, ch 10 data).

With the 14th channel of the subject's pipeline results, how baseline fluctuations corrected can be seen in figure 4.6 and figure 4.7.

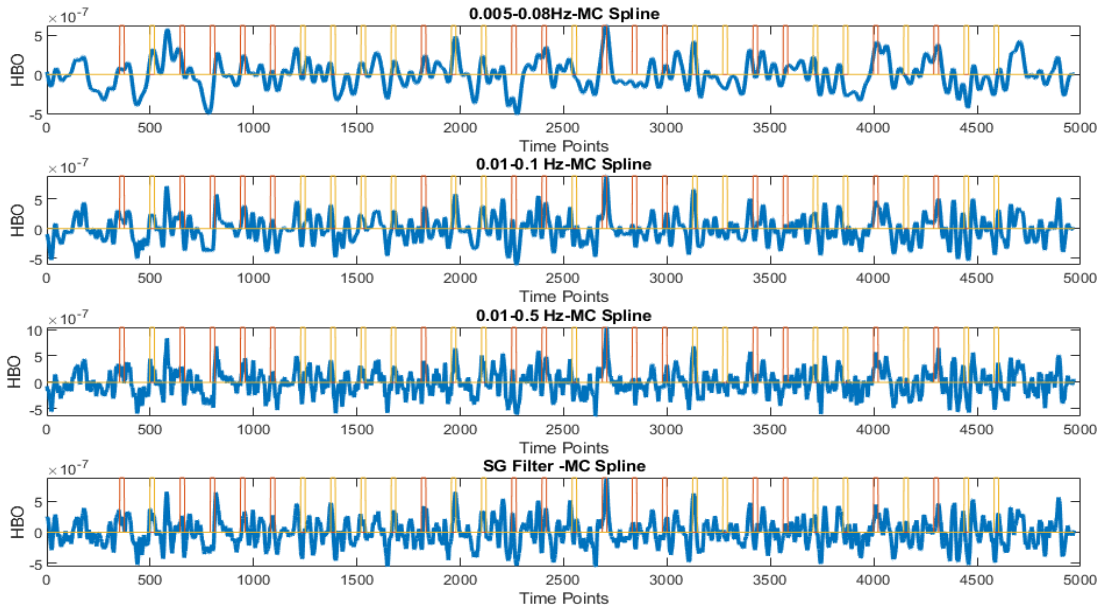

Figure 4.6. Visualization of the impact of different cut-off frequencies on data corrected with Spline Interpolation (Subject 1 Ch 14 data).

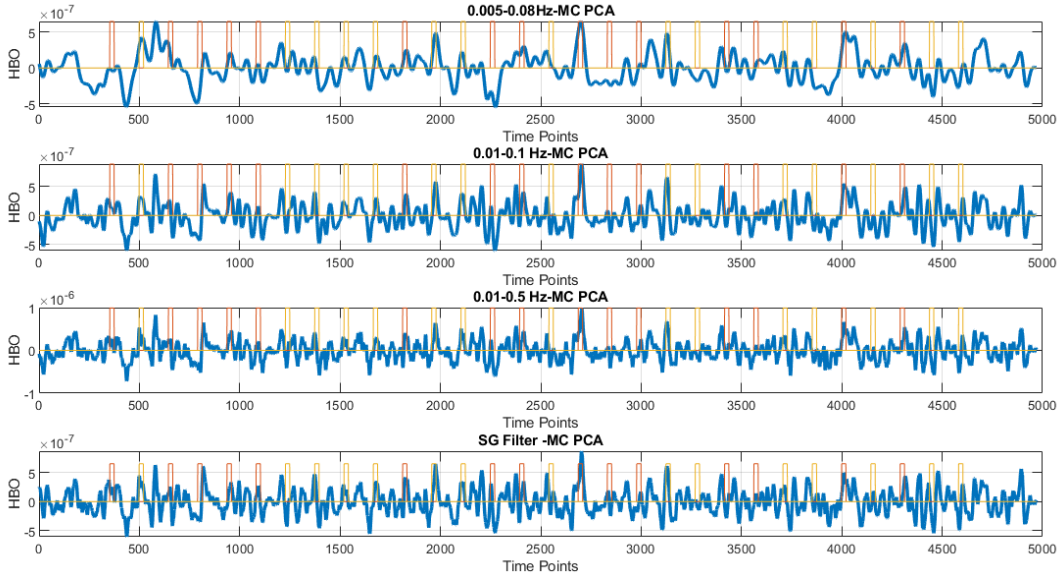

Figure 4.7. Visualization of the impact of different cut-off frequencies on data corrected with PCA -Subject 1 ch 14 data.

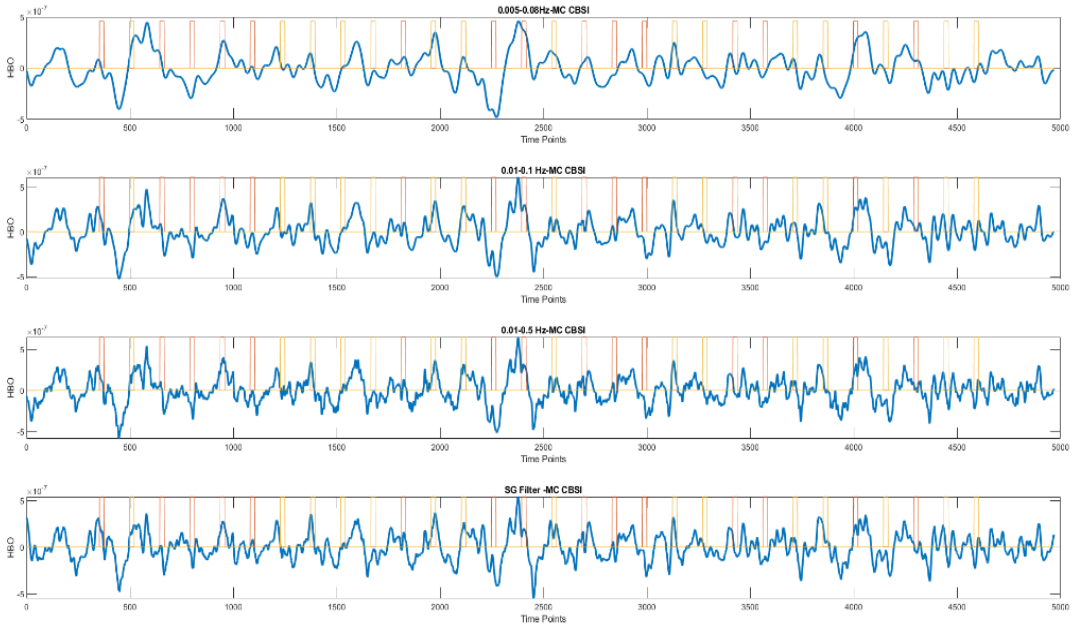

Figure 4.8. Visualization of the impact of different cut-off frequencies on data corrected with CBSI-Subject 1 Channel 14.

Comparison of Different Preprocessing Strategies on Block Averaged HBO Data

Figure 4.9 demonstrates the impact of each LF denoising technique (i.e., PCA 75, PCA 90, PCA 1st, none) on HBO time series data motion corrected with PCA and bandpass filtered with different options. HBO Data is from Channel 10 and is block averaged across all Pain trials of subject 1. Similarly, the impact of each LF denoising technique on HBO time series data which are bandpass filtered with different filter options can be visualized in Figures 4.10 and 4.11 for Spline and CBSI motion correction methods. How different preprocessing pipelines resulted in significantly different waveforms is worth notice.

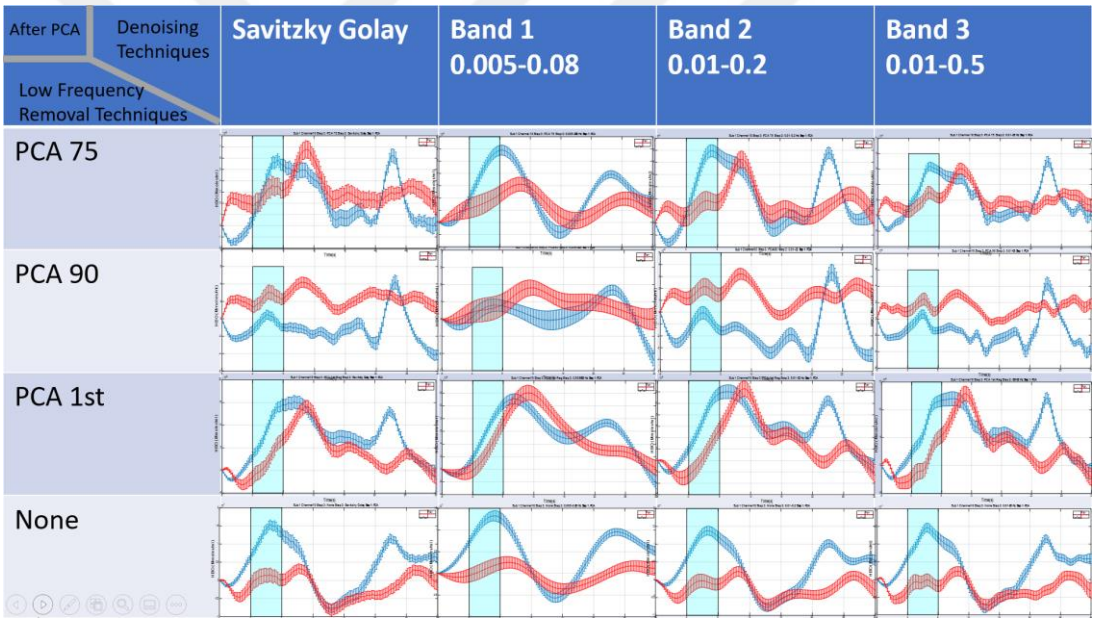

Figure 4.9. Pipeline Comparison: After PCA motion correction method.

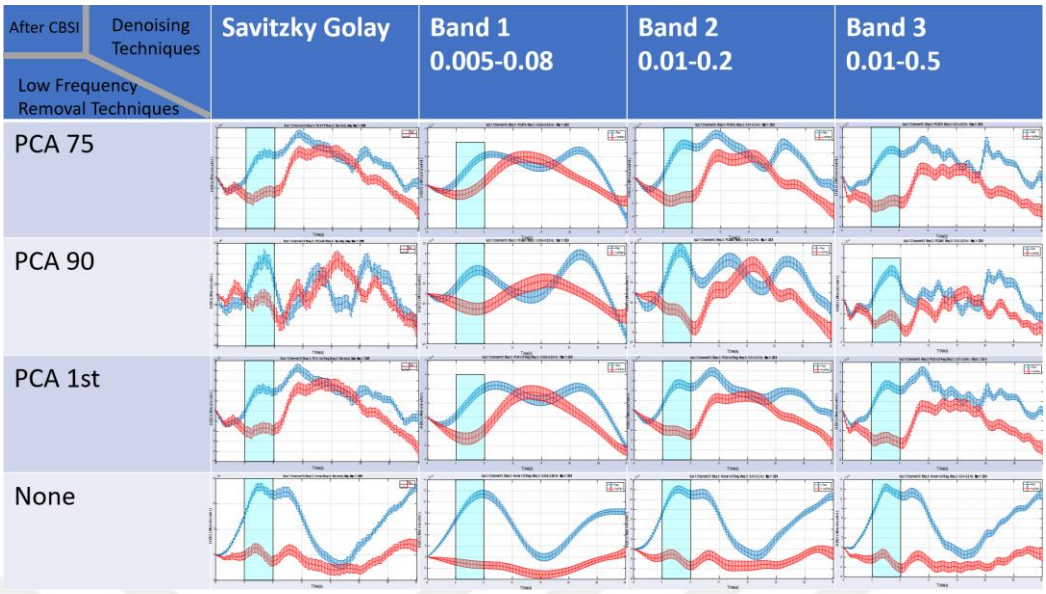

Figure 4.10. Pipeline Comparison: After CBSI motion correction method.

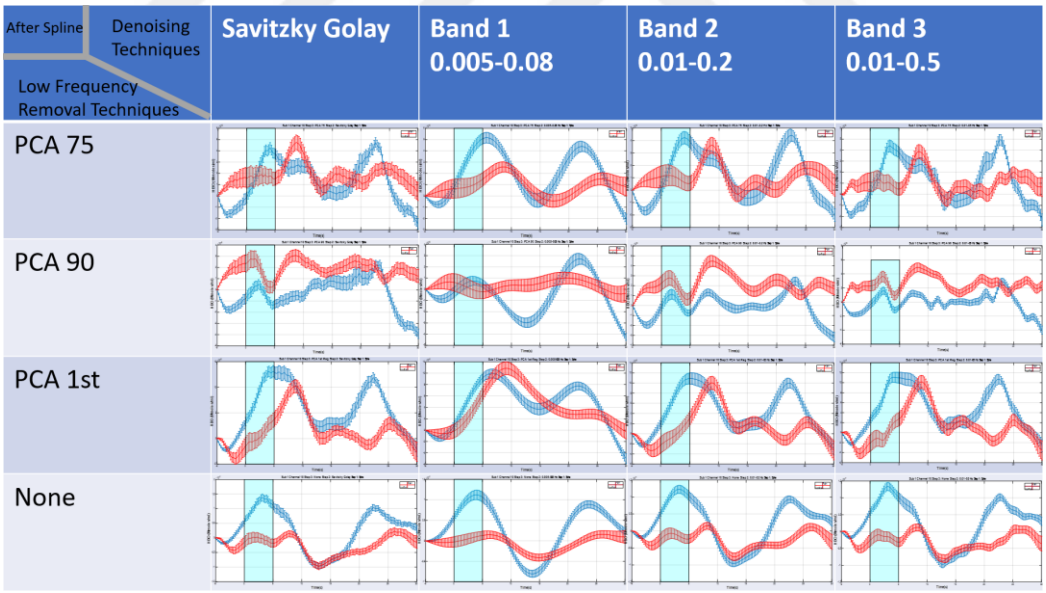

Figure 4.11. Pipeline Comparison: After the Spline motion correction method.

Evaluation of performance metrics

As stated in the methods section, performance of each noise removal pipeline was evaluated by several metrics that describe the quality of the denoised signal in terms of how well it fits to a model stimulus. These metrics were trial to trial variability, SNR, CNR, Cohen's d, a parameter describing activation strength (PAR), beta weights from GLM, t values for each contrast condition (e.g., Pain>0, Pain>NonPain) derived from GLM, mean squared error (MSE) and correlation with stimulus pattern (R). In order to test performance with these metrics, first a region of interest (ROI) which would remain robustly active after application of a majority of the preprocessing strategies was determined. Then, the signal quality in this ROI was compared after application of all preprocessing methods.

ROI selection

As a first step for evaluating the performance metrics for all pipelines, T stats was applied on different performance metrics for pain>0 and pain > non-pain stimuli conditions. The t statistics for all channels and methods were computed for each performance parameter as demonstrated in Fig 4.12.

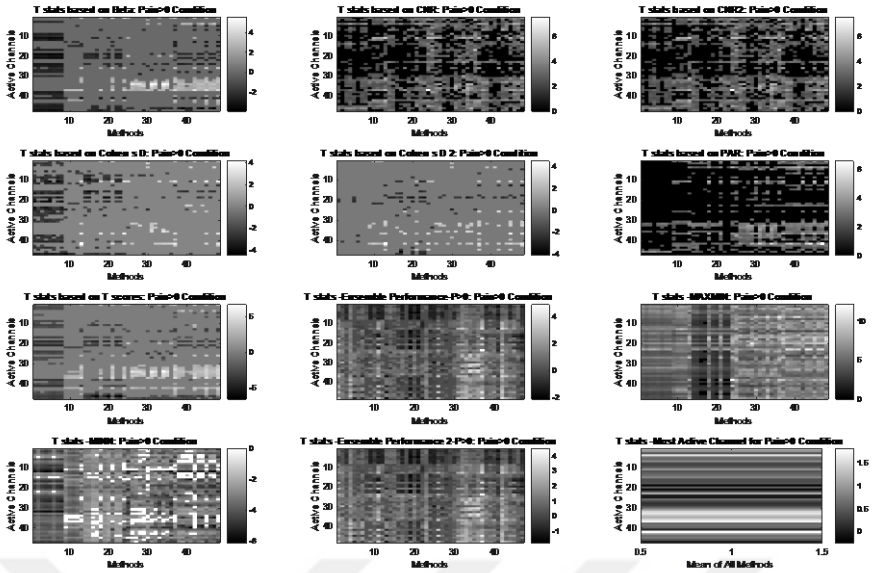

Figure 4.12. T stats for pain>0 condition for all metrics.

The most active channel was found to be Channel 42 (SMC) for Pain >0 condition when all t maps were combined in a single parameter map (Figure 4.13). The performance of each metric was computed for this channel ROI.

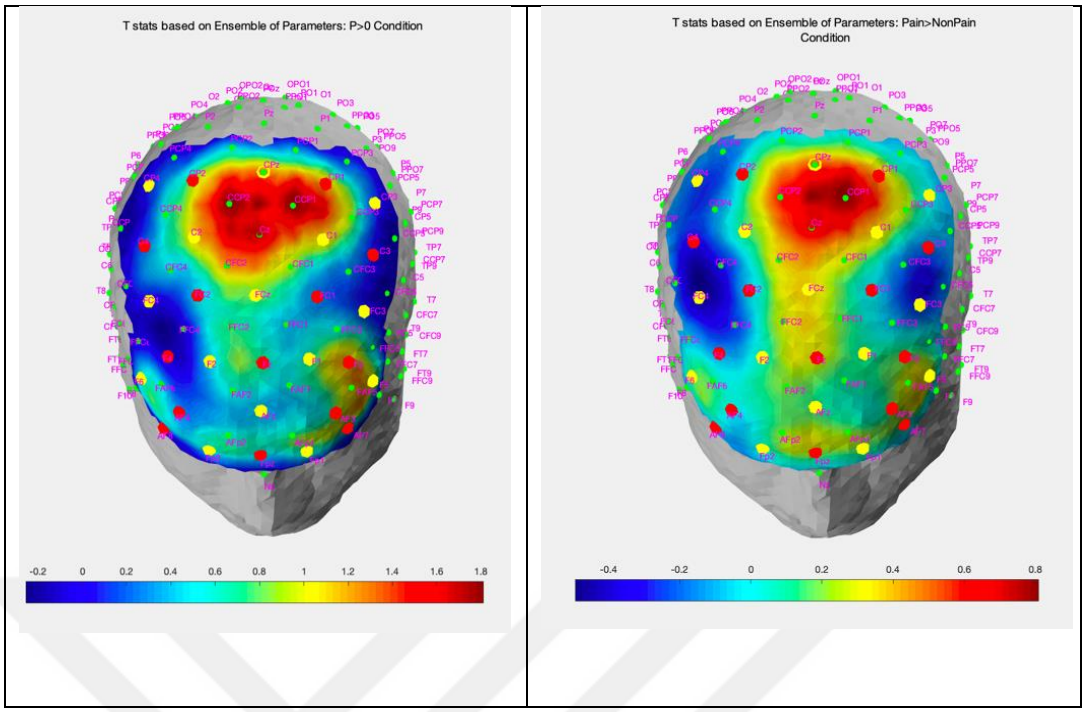

Figure 4.13. Group Level Activation Map for p>0 and p>np conditions.

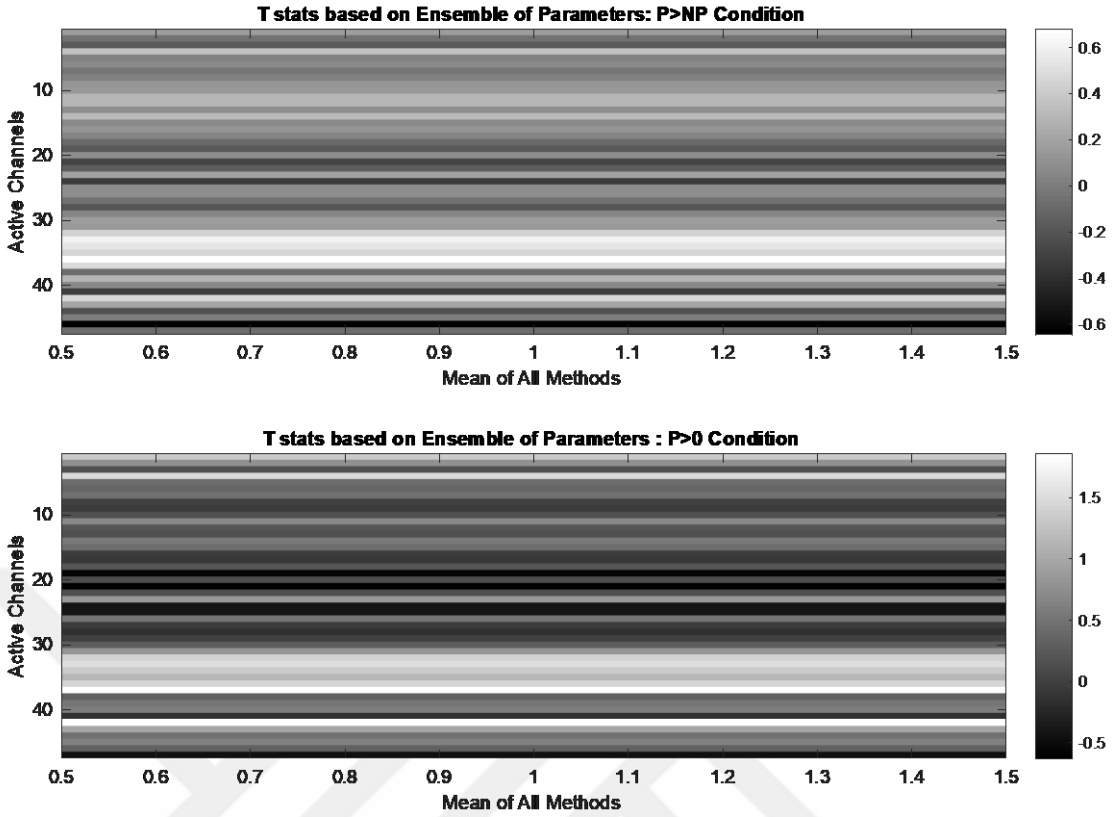

Figure. 4.14. ROI selection was performed by choosing channels that would remain active for a majority of the methods and activation parameters. Improvements in signal quality for this ROI was then assessed with different methods.

Figure 4.15 qualitatively shows the group level performance of each activation parameter in Channel 42 for 48 preprocessing pipelines.

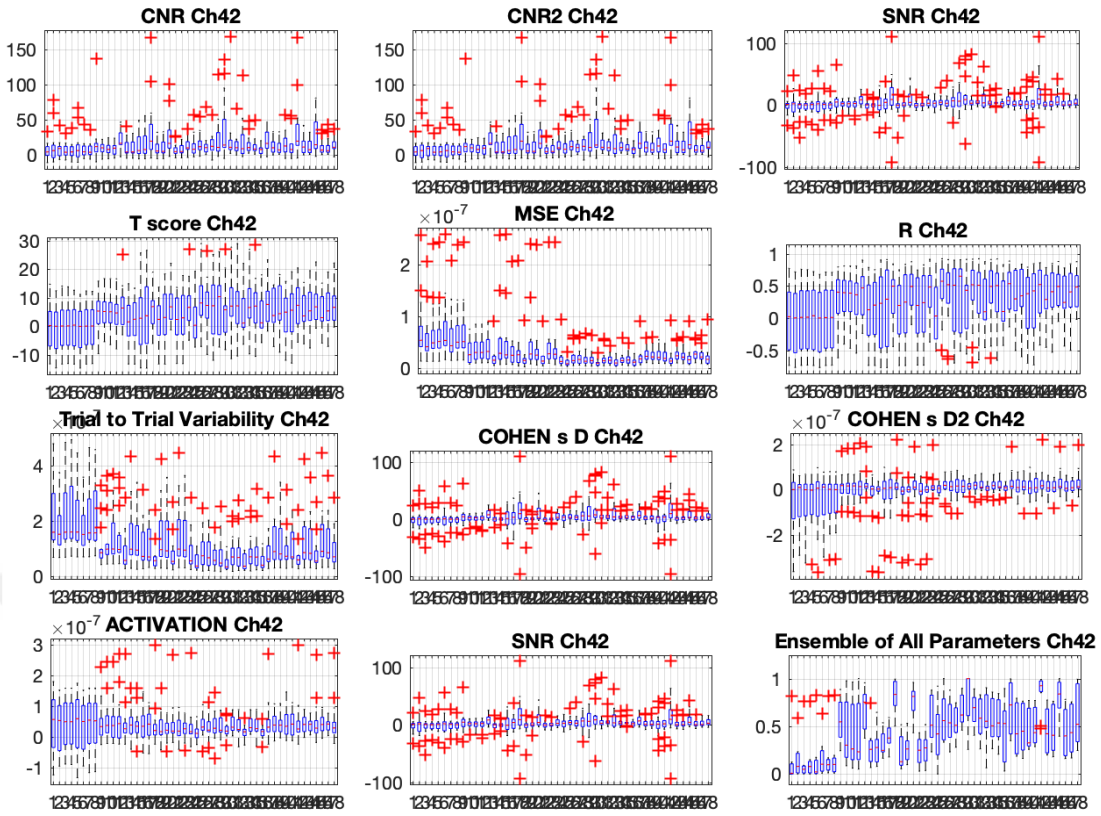

Figure 4.15. Box car plots showing the performance of each activation parameter for all preprocessing pipelines (x axis). Each box plot shows the median (line and notch), the 25th and 75th percentiles (the edges of each box) and the most extreme values not considered outliers (whiskers). Performance metrics are: CNR (computed with two different formulas), T score, trial to trial variability, SNR, Cohen's d (computed with two different formulas), MSE and R with model stimulus pattern derived from GLM. All performance metrics were combined into a single parameter in order to derive the optimal preprocessing strategy.

The performance of each metric was then normalized by scaling between maximum and minimum values of that parameter across all methods. All normalized parameters were combined into a single performance parameter by taking the mean for each preprocessing pipeline.

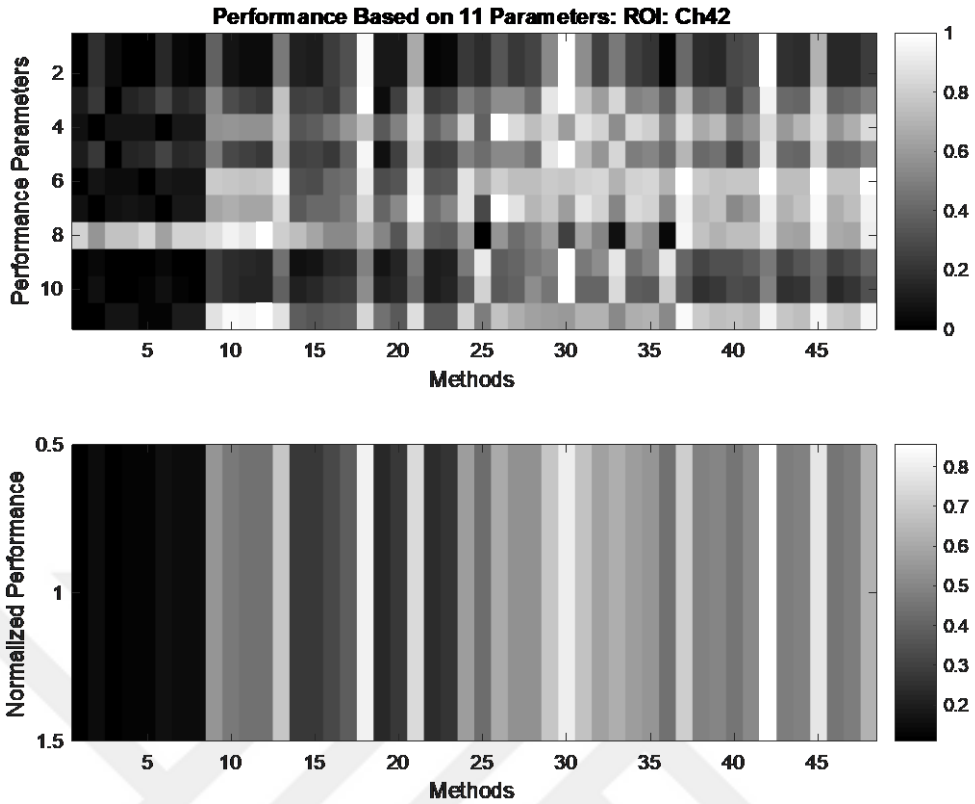

Figure 4.16 Each performance metric was normalized between 0 and 1.

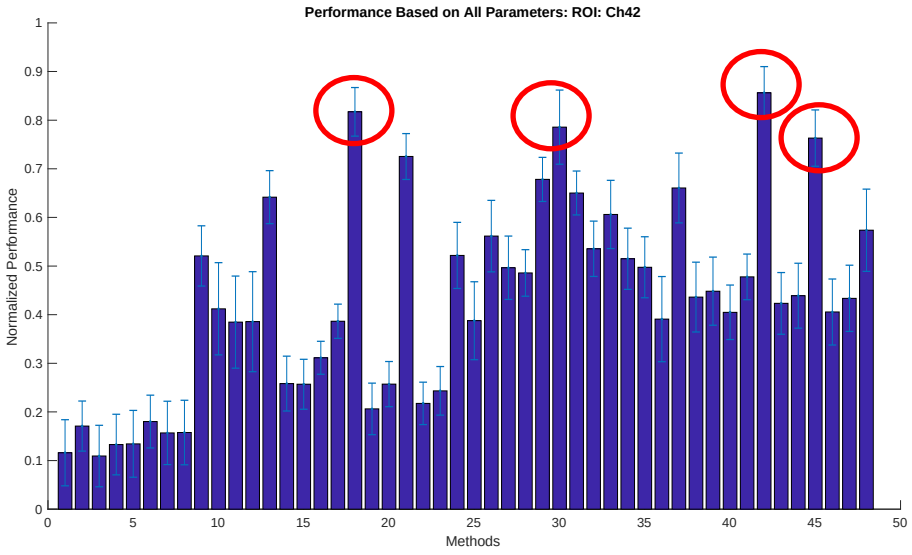

Figure 4.17. Bar plots showing the normalized performance of all metrics for all preprocessing pipelines.

Table 4.1. The top 5 best performer pipelines and the lowest 5 performer pipelines were selected for comparison.

Performers	Method Selection	
	Highest performers	**Lowest Performers**
Method no (MC, BP, LF)	**1.** #45 (CBSI, 0.01-0.2Hz, PCA1st)	**1.** #1 (PCA, Savitzky Golay, None)
	2. #30 (CBSI,0.005-0.08Hz,PCA90)	**2.** #3 (PCA, 0.01Hz- 0.2 Hz, None)
	3. #18 (CBSI,0.005-0.08Hz,PCA75)	**3.** #4 (PCA, 0.01Hz- 0.5 Hz, None)
	4. #42 (CBSI,0.005-0.08Hz,PCA75)	**4.** #5 (Spline, Savitzky Golay, None)

The best preprocessing pipeline that improved signal quality the most, included the following steps: 1) motion correction performed by CBSI , 2) band pass filtering with Butteroworth Filter to the frequency range of 0.01-0.2 Hz and 3) removal of common physiological fluctuations in all channels by regressing out the first principal component derived from PCA analysis.

The same procedure was applied to cognitive data collected from elderly adults during a word processing task which included 4 different conditions (presentation of literal words, novel words, abnormal words and conventional words), the details of which can be found in the Appendix section. The best preprocessing practices were listed as follows:

Table 4.2. The top 5 best performer pipelines and the lowest 5 performer pipelines were selected for comparison.

Performers	Method Selection	
	Highest performers	**Lowest Performers**
Method no (MC, BP, LF)	**1.** #9 (CBSI, 0.005-0.08Hz, None)	**1.** #27 (Spline, Savitzky Golay, PCA90)
	2. #6 (Spline,0.005-0.08Hz,None)	**2.** #26 (PCA, Savitzky Golay, PCA90)
	3. #2 (PCA,0.005-0.08Hz,None)	**3.** #34 (PCA, 0.01Hz- 0.5 Hz, PCA90)
	4. #40 (PCA,0.005-0.08Hz, PCA^{1st})	**4.** #36 (CBSI, 0.01Hz- 0.5 Hz, PCA90)

5. CONCLUSION

The aim of this study was to present a systematic comparison of several different preprocessing pipelines which were created by concatenating the most commonly applied methods in FNIRS literature for motion correction, band pass filtering and low frequency systemic noise removal.

Throughout the last decade, many different denoising methods and motion correction techniques were applied to FNIRS data for improving signal quality. However; no golden standard method was implemented among majority of the groups. Some filtering was inadequate to remove noise components while others could degrade the activation signal. In this study, the effect of frequently used filters on data was investigated and compared to find the best method. For motion correction, CBSI, PCA and Spline methods were tested. CBSI came out to be the most effective method for removal of motion artifacts. In addition to these motion correction techniques, the recursive PCA, the hybrid Savitzky Golay and Spline Interpolation techniques were also tested. The Savitzky Golay & Spline interpolation Hybrid method has been set aside for error in subject 8 data. These filters will be systematically tested for future work. In this study, only the main motion correction techniques, which can be considered as basic, were used. On the other hand, wavelet filtering is also one of the most common motion correction technique. Since PCA was found to be more effective in spike and baseline shifts in the literature, PCA was used instead of the wavelet algorithm.

Short channel separation could not be used in our study because of hardware limitations. 3 different bandpass filter ranges were used for isolating frequencies of interest where the neuronal activity related hemodynamic responses reside. These were determined by examining the most frequently cited works in FNIRS literature and their results. In addition, the Savitzky Golay technique, whose effect is similar to Bandpass

2 (0.01-0.2Hz), was tested. 3 different PCA methods were further utilized to remove low frequency systemic physiological noise.

Similarly, to the motion artifact correction version, PCA can be used to remove low frequency systemic interference as systematic fluctuations are covariant among FNIRS measurements from different channels. Causing a decrease in covariance can eliminate low-frequency physiological noises from the data (13). In addition, no low frequency noise removal option has been added to test whether these filters have a negative effect on hemodynamic response.

T statistics has been done to find the most active channels that can provide the same Pain> Nonpain condition for all of these parameters. After obtaining those channels that attitude metrics, we decided to find the best and worst performer methods by focusing on the data of one of those channels (channel 12).

While many studies have emphasized the severity of physiological noise, no golden standard preprocessing technique could be proposed for eliminating systemic physiological artifacts which overlay hemodynamic signals induced by neuronal activation. Several methods for removal of systemic and motion artifacts from FNIRS signals have been proposed in the literature. However; no standardized pipeline of preprocessing steps could be reliably proposed as a gold standard for isolating the task related neuronally induced hemodynamic changes of interest. The aim of this study was to implement commonly applied noise reduction strategies in FNIRS literature into varying preprocessing pipelines and compare the performance of 48 different pipelines in increasing the signal to noise ratio in FNIRS signal collected during motor tasks. The best performer method for denoising motor cortex data was found to be Method 45 which included the following steps: 1) motion correction performed by CBSI , 2) band pass filtering with Butteroworth Filter to the frequency range of 0.01-

0.2 Hz and 3) removal of common physiological fluctuations in all channels by regressing out the first principal component derived from PCA analysis.

The purpose of this study was to provide a visual reference showing the effects of different processing methods, to help inform researchers in setting up and evaluating a processing pipeline. We show the significant impact of pre- and post-processing choices. Optimum processing methods have not been established among FNIRS community, however in this study we propose a method for determining an active ROI depending on the type of experimental paradigm and channels used which would remain active after application of a majority of methods. Next, we evaluate the performance of 48 different pipelines on improving the signal quality in this ROI among all subject data. Our methodology presents a novel and practical automated selection for the best preprocessing practices for different NIRS data sets.

BIBLIOGRAPHY

1. Pinti P, Scholkmann F, Hamilton A, Burgess P, Tachtsidis I. Current status and issues regarding pre-processing of FNIRS neuroimaging data: An investigation of diverse signal filtering methods within a General Linear Model framework. Frontiers in human neuroscience. 2018;12:505.
2. Biasiucci A, Franceschiello B, Murray MM. Electroencephalography. Current Biology. 2019 Feb 4;29(3):R80-5.
3. Kao C, Zhang Y. Magnetic Source Imaging and Infant MEG: Current Trends and Technical Advances. Brain sciences. 2019 Aug;9(8):181.
4. Glover, Gary H. "Overview of functional magnetic resonance imaging." Neurosurgery Clinics 22.2 2011: 133-139.
5. Yücel MA, Selb JJ, Huppert TJ, Franceschini MA, Boas DA. Functional near infrared spectroscopy: Enabling routine functional brain imaging. Current opinion in biomedical engineering. 2017 Dec 1;4:78-86.
6. Huneau C, Benali H, Chabriat H. Investigating human neurovascular coupling using functional neuroimaging: a critical review of dynamic models. Frontiers in neuroscience. 2015 Dec 18;9:467.
7. Scholkmann F, Kleiser S, Metz AJ, Zimmermann R, Pavia JM, Wolf U, Wolf M. A review on continuous wave functional near-infrared spectroscopy and imaging instrumentation and methodology. Neuroimage. 2014 Jan 15;85:6-27.
8. Khan RA, Naseer N, Qureshi NK, Noori FM, Nazeer H, Khan MU. FNIRS-based Neurorobotic Interface for gait rehabilitation. Journal of neuroengineering and rehabilitation. 2018 Dec;15(1):7.
9. Ferrari M, Quaresima V. A brief review on the history of human functional near-infrared spectroscopy (FNIRS) development and fields of application. Neuroimage. 2012 Nov 1;63(2):921-35.
10. Kohno S, Miyai I, Seiyama A, Oda I, Ishikawa A, Tsuneishi S, Amita T, Shimizu K. Removal of the skin blood flow artifact in functional near-infrared spectroscopic imaging data through independent component analysis. Journal of biomedical optics. 2007 Nov;12(6):062111.
11. Zimmermann R, Marchal-Crespo L, Edelmann J, Lambercy O, Fluet MC, Riener R, Wolf M, Gassert R. Detection of motor execution using a hybrid FNIRS-biosignal BCI: a feasibility study. Journal of neuroengineering and rehabilitation. 2013 Dec;10(1):4.
12. Sulzer J, Haller S, Scharnowski F, Weiskopf N, Birbaumer N, Blefari ML, Bruehl AB, Cohen LG, DeCharms RC, Gassert R, Goebel R. Real-time fMRI neurofeedback: progress and challenges. Neuroimage. 2013 Aug 1;76:386-99.
13. Naseer N, Hong KS. FNIRS-based brain-computer interfaces: a review. Frontiers in human neuroscience. 2015 Jan 28;9:3.
14. Boas DA, Gaudette T, Strangman G, Cheng X, Marota JJ, Mandeville JB. The accuracy of near infrared spectroscopy and imaging during focal changes in cerebral hemodynamics. Neuroimage.

2001 Jan 1;13(1):76-90.

15. Pinti P, Scholkmann F, Hamilton A, Burgess P, Tachtsidis I. Current status and issues regarding pre-processing of FNIRS neuroimaging data: An investigation of diverse signal filtering methods within a General Linear Model framework. Frontiers in human neuroscience. 2018;12:505.
16. Patil AV, Safaie J, Moghaddam HA, Wallois F, Grebe R. Experimental investigation of NIRS spatial sensitivity. Biomedical optics express. 2011 Jun 1;2(6):1478-93.
17. Yücel MA, Selb J, Aasted CM, Lin PY, Borsook D, Becerra L, Boas DA. Mayer waves reduce the accuracy of estimated hemodynamic response functions in functional near-infrared spectroscopy. Biomedical optics express. 2016 Aug 1;7(8):3078-88.
18. Huppert TJ, Diamond SG, Franceschini MA, Boas DA. HomER: a review of time-series analysis methods for near-infrared spectroscopy of the brain. Applied optics. 2009 Apr 1;48(10):D280-98.
19. Franceschini MA, Fantini S, Thompson JH, Culver JP, Boas DA. Hemodynamic evoked response of the sensorimotor cortex measured noninvasively with near-infrared optical imaging. Psychophysiology. 2003 Jul;40(4):548-60.
20. Gratton G, Brumback CR, Gordon BA, Pearson MA, Low KA, Fabiani M. Effects of measurement method, wavelength, and source-detector distance on the fast optical signal. Neuroimage. 2006 Oct 1;32(4):1576-90.
21. Power SD, Falk TH, Chau T. Classification of prefrontal activity due to mental arithmetic and music imagery using hidden Markov models and frequency domain near-infrared spectroscopy. Journal of neural engineering. 2010 Feb 18;7(2):026002.
22. Luu S, Chau T. Decoding subjective preference from single-trial near-infrared spectroscopy signals. Journal of neural engineering. 2008 Dec 22;6(1):016003.
23. Naseer N, Hong MJ, Hong KS. Online binary decision decoding using functional near-infrared spectroscopy for the development of brain–computer interface. Experimental brain research. 2014 Feb 1;232(2):555-64.
24. Liu, Y., et al. "Foundations of Augmented Cognition." 2013.
25. Hu XS, Hong KS, Ge SS. FNIRS-based online deception decoding. Journal of Neural Engineering. 2012 Feb 16;9(2):026012.
26. Hu XS, Hong KS, Ge SS. Recognition of stimulus-evoked neuronal optical response by identifying chaos levels of near-infrared spectroscopy time series. Neuroscience letters. 2011 Oct 24;504(2):115-20.
27. Tomita Y, Vialatte FB, Dreyfus G, Mitsukura Y, Bakardjian H, Cichocki A. Bimodal BCI using simultaneously NIRS and EEG. IEEE Transactions on Biomedical Engineering. 2014 Jan 16;61(4):1274-84.
28. Tachtsidis I, Scholkmann F. False positives and false negatives in functional near-infrared spectroscopy: issues, challenges, and the way forward. Neurophotonics. 2016 Mar;3(3):031405.
29. Tachtsidis I, Koh PH, Stubbs C, Elwell CE. Functional optical topography analysis using statistical parametric mapping (SPM) methodology with and without physiological confounds. InOxygen Transport to Tissue XXXI 2010 (pp. 237-243). Springer, Boston, MA.

30. Zhang Y, Brooks DH, Franceschini MA, Boas DA. Eigenvector-based spatial filtering for reduction of physiological interference in diffuse optical imaging. Journal of biomedical optics. 2005 Jan;10(1):011014.
31. Zhang Q, Brown EN, Strangman GE. Adaptive filtering to reduce global interference in evoked brain activity detection: a human subject case study. Journal of biomedical optics. 2007 Nov;12(6):064009.
32. Zhang Q, Strangman GE, Ganis G. Adaptive filtering to reduce global interference in non-invasive NIRS measures of brain activation: how well and when does it work?. Neuroimage. 2009 Apr 15;45(3):788-94..
33. Li Y, Zhang H, Yu M, Yu W, Frederick BD, Tong Y. Systemic low-frequency oscillations observed in the periphery of healthy human subjects. Journal of biomedical optics. 2018 May;23(5):057001.
34. Izzetoglu M, Devaraj A, Bunce S, Onaral B. Motion artifact cancellation in NIR spectroscopy using Wiener filtering. IEEE Transactions on Biomedical Engineering. 2005 Apr 18;52(5):934-8.
35. Nguyen HT, Ngo CQ, Truong Quang Dang KH, Vo VT. Temporal hemodynamic classification of two hands tapping using functional near—infrared spectroscopy. Frontiers in human neuroscience. 2013 Sep 2;7:516.
36. Shin J, Jeong J. Multiclass classification of hemodynamic responses for performance improvement of functional near-infrared spectroscopy-based brain–computer interface. Journal of biomedical optics. 2014 Jun;19(6):067009.
37. Power SD, Kushki A, Chau T. Towards a system-paced near-infrared spectroscopy brain–computer interface: differentiating prefrontal activity due to mental arithmetic and mental singing from the no-control state. Journal of neural engineering. 2011 Oct 6;8(6):066004.
38. Power SD, Kushki A, Chau T. Intersession consistency of single-trial classification of the prefrontal response to mental arithmetic and the no-control state by NIRS. PloS one. 2012 Jul 23;7(7):e37791.
39. Santosa H, Jiyoun Hong M, Kim SP, Hong KS. Noise reduction in functional near-infrared spectroscopy signals by independent component analysis. Review of Scientific Instruments. 2013 Jul 10;84(7):073106.
40. Zhang Y, Brooks DH, Franceschini MA, Boas DA. Eigenvector-based spatial filtering for reduction of physiological interference in diffuse optical imaging. Journal of biomedical optics. 2005 Jan;10(1):011014.
41. Boas DA, Dale AM, Franceschini MA. Diffuse optical imaging of brain activation: approaches to optimizing image sensitivity, resolution, and accuracy. Neuroimage. 2004 Jan 1;23:S275-88.
42. Cooper R, Selb J, Gagnon L, Phillip D, Schytz HW, Iversen HK, Ashina M, Boas DA. A systematic comparison of motion artifact correction techniques for functional near-infrared spectroscopy. Frontiers in neuroscience. 2012 Oct 11;6:147.
43. Franceschini MA, Fantini S, Thompson JH, Culver JP, Boas DA. Hemodynamic evoked response of the sensorimotor cortex measured noninvasively with near-infrared optical imaging. Psychophysiology. 2003 Jul;40(4):548-60.
44. Sato T, Nambu I, Takeda K, Aihara T, Yamashita O, Isogaya Y, Inoue Y, Otaka Y, Wada Y, Kawato

M, Sato MA. Reduction of global interference of scalp-hemodynamics in functional near-infrared spectroscopy using short distance probes. NeuroImage. 2016 Nov 1;141:120-32.

45. Scholkmann F, Spichtig S, Muehlemann T, Wolf M. How to detect and reduce movement artifacts in near-infrared imaging using moving standard deviation and spline interpolation. Physiological measurement. 2010 Mar 22;31(5):649.
46. Arendt-Nielsen L, Nie H, Laursen MB, Laursen BS, Madeleine P, Simonsen OH, Graven-Nielsen T. Sensitization in patients with painful knee osteoarthritis. Pain. 2010 Jun 1;149(3):573-81.
47. Hocke L, Oni I, Duszynski C, Corrigan A, Frederick B, Dunn J. Automated Processing of FNIRS Data—a visual guide to the pitfalls and consequences. Algorithms. 2018 May;11(5):67.

APPENDIX

COGNITIVE DATA

ROI Selection

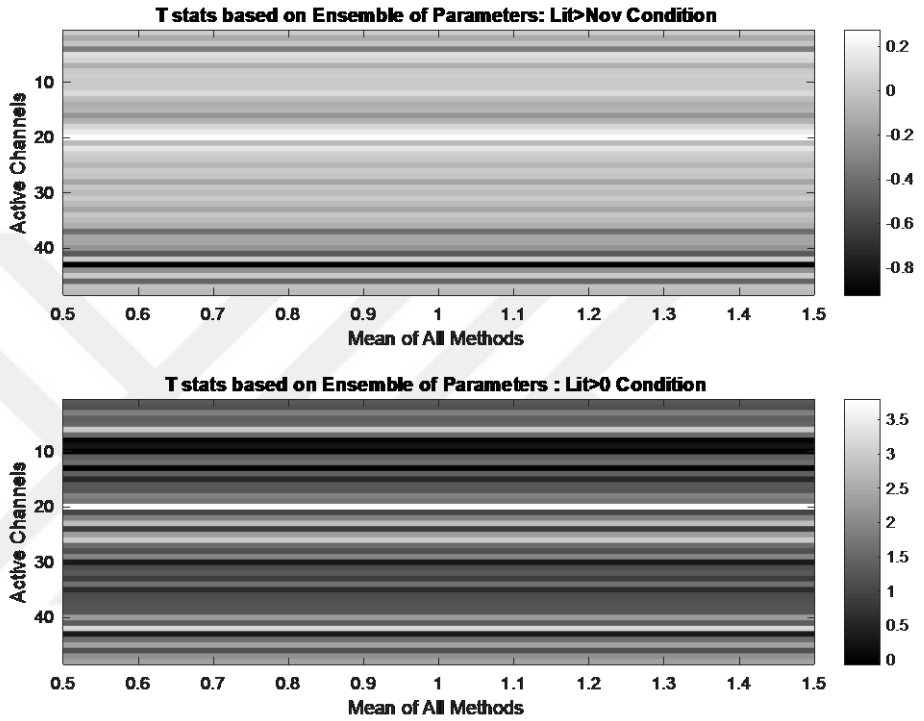

ROI Selection

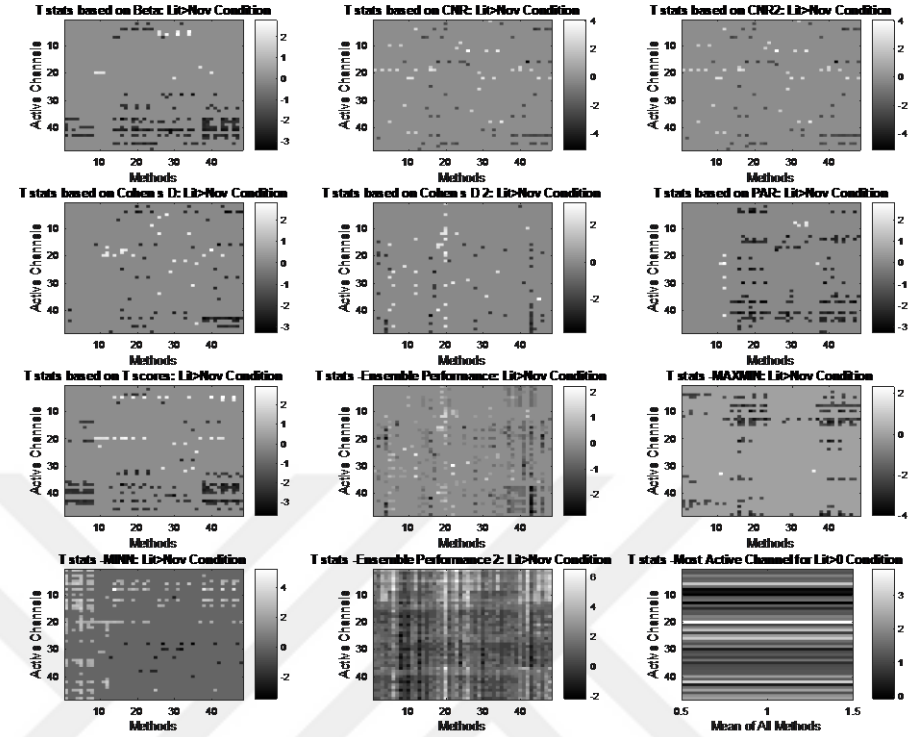

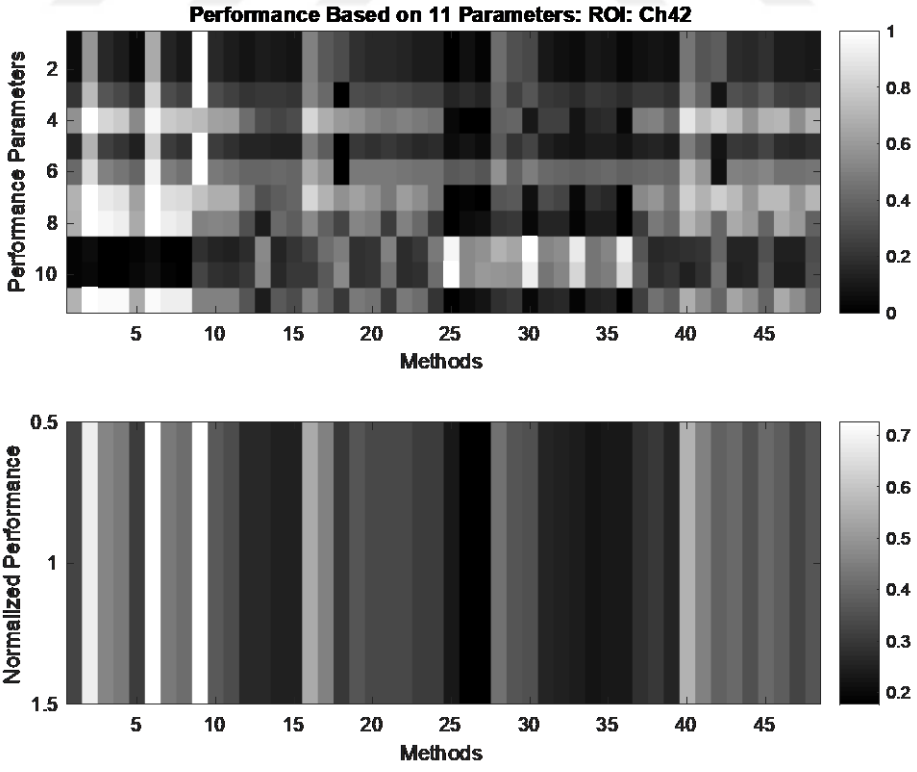

Bar plots showing the normalized performance of all metrics for all preprocessing pipelines.

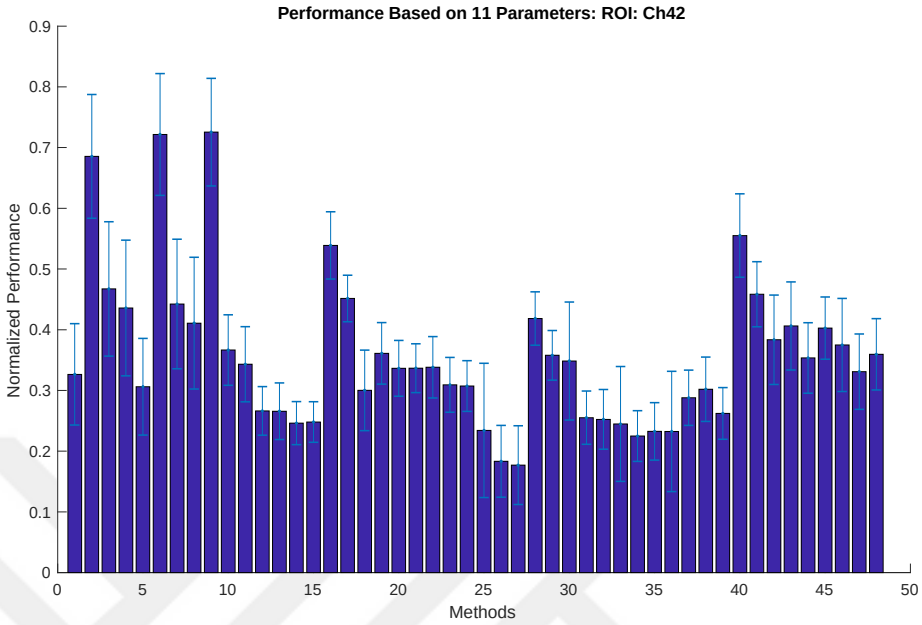

Box car plots showing the performance of each activation parameter for all preprocessing pipelines (x axis).

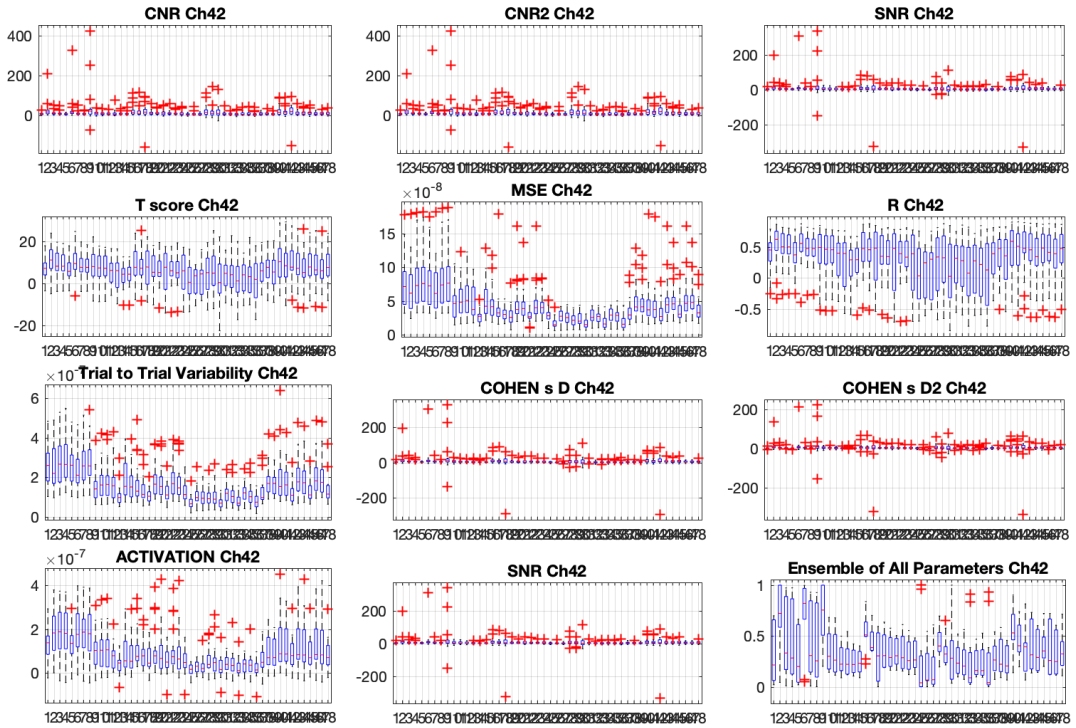

Hemodynamic response in different channels.

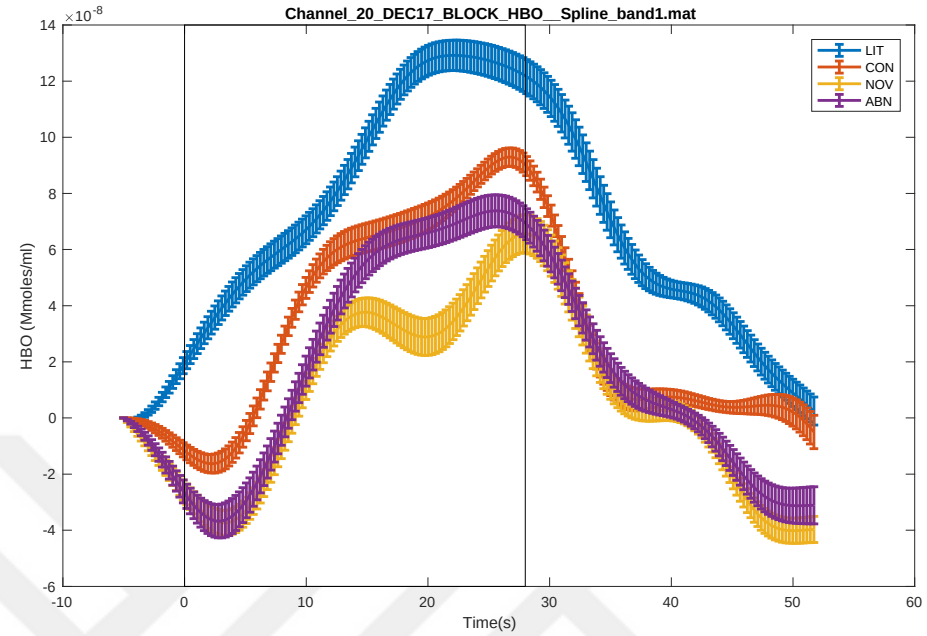

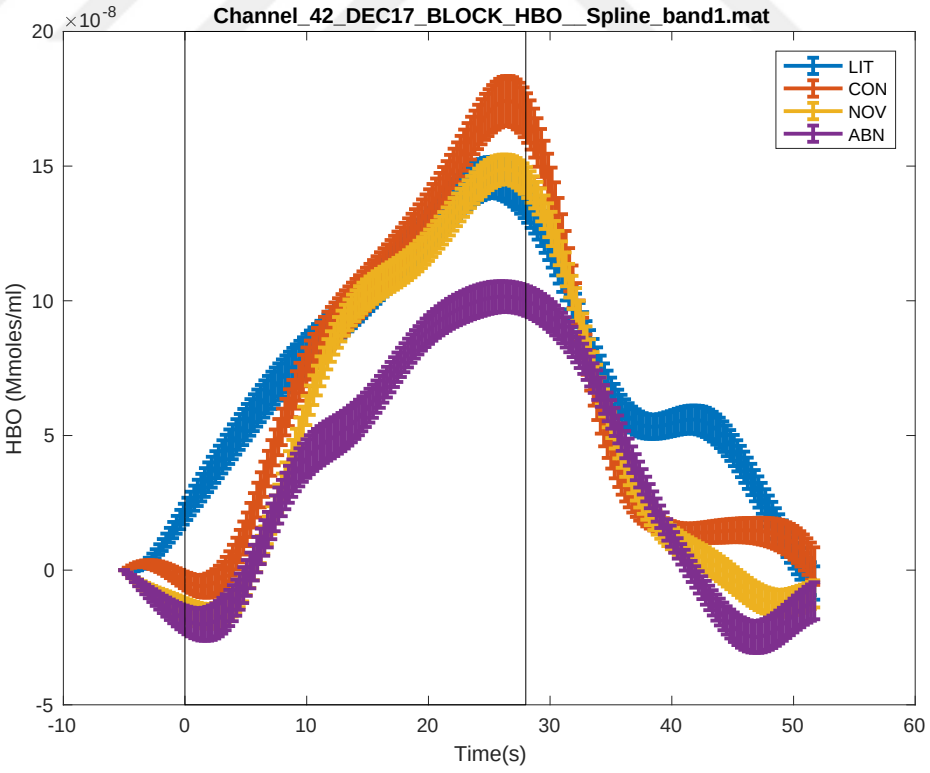

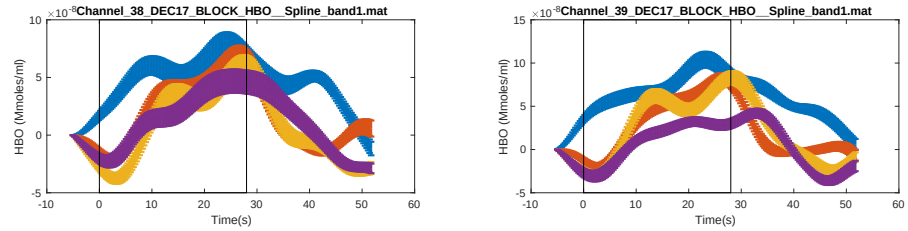
Channel_38_DEC17_BLOCK_HBO__Spline_band1.mat
Channel_39_DEC17_BLOCK_HBO__Spline_band1.mat
HBO (Mmoles/ml)
Time(s)

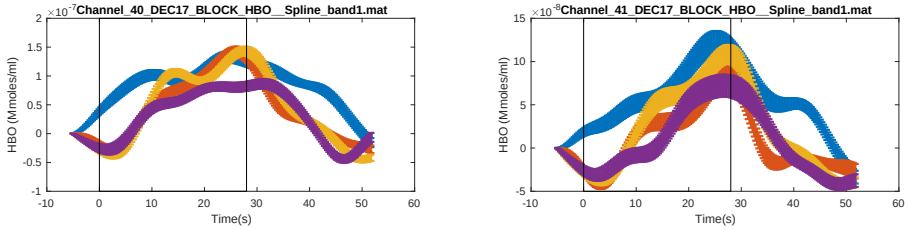
Channel_40_DEC17_BLOCK_HBO__Spline_band1.mat
Channel_41_DEC17_BLOCK_HBO__Spline_band1.mat
HBO (Mmoles/ml)
Time(s)

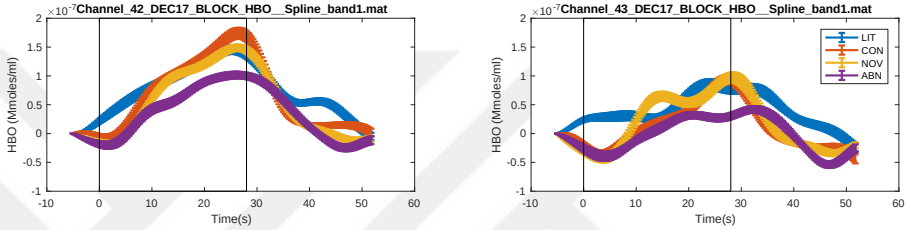
Channel_42_DEC17_BLOCK_HBO__Spline_band1.mat
Channel_43_DEC17_BLOCK_HBO__Spline_band1.mat
LIT
CON
NOV
ABN
HBO (Mmoles/ml)
Time(s)

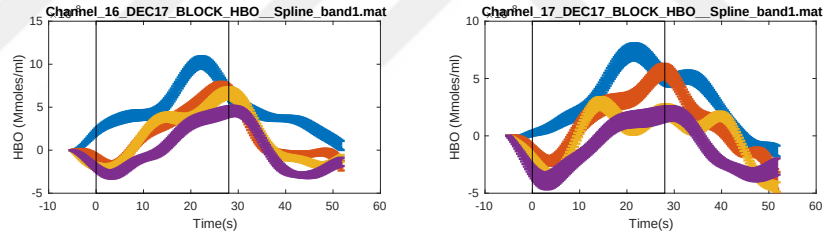
Channel_16_DEC17_BLOCK_HBO__Spline_band1.mat
Channel_17_DEC17_BLOCK_HBO__Spline_band1.mat
HBO (Mmoles/ml)
Time(s)

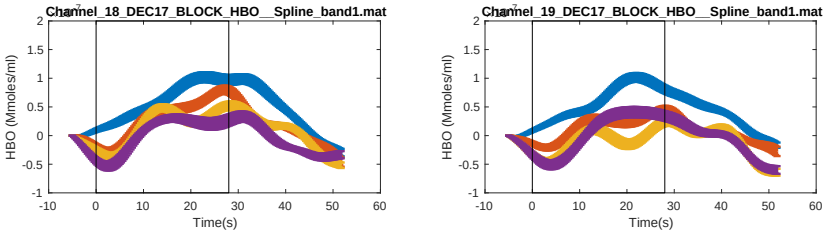
Channel_18_DEC17_BLOCK_HBO__Spline_band1.mat
Channel_19_DEC17_BLOCK_HBO__Spline_band1.mat
HBO (Mmoles/ml)
Time(s)

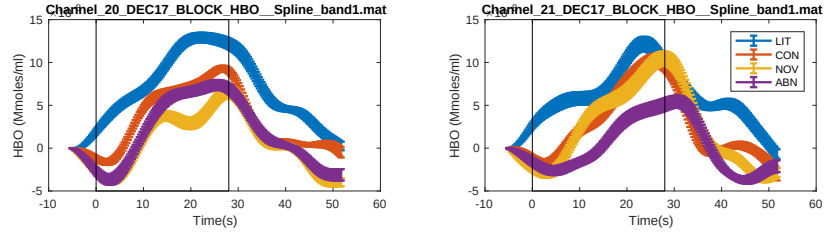
Channel_20_DEC17_BLOCK_HBO__Spline_band1.mat
Channel_21_DEC17_BLOCK_HBO__Spline_band1.mat
LIT
CON
NOV
ABN
HBO (Mmoles/ml)
Time(s)

RESUME

Personal Information

Name	Umut	**Surname**	Karadeniz
Birth Place	Istanbul	**Birth Day**	06/06/1994
Nationality	T.C	**Phone Number**	+905457197775
E-mail	umut.karadeniz@yahoo.com		

Education

	Institution	**Graduation Year**
Undergraduate	Yeditepe University	2016
High School	Buyuksehir Huseyin Yildiz Anatolian High School	2012

Experience

Position	**Organization**	**Duration (Year – Year)**
Business Developer	ICFO Research Institute	2019-Present
Management Trainee	Acibadem Technology	2016-2018
Product Specialist	DIRUI Turkey	2016-2016

Language	**Reading**	**Speaking**	**Writing**
English	Very Good	Very Good	Very Good
Spanish	Intermediate	Intermediate	Intermediate

Foreign Language Examination Grade									
KPDS	ÜDS	IELTS	TOEFL	TOEFL IBT	TOEFL CBT	CAE	CPE	YÖKDİL	YDS

KPDS: Kamu Personeli Yabancı Dil Sınavı; ÜDS: Üniversitelerarası Kurul Yabancı Dil Sınavı; IELTS: International English Language Testing System; TOEFL IBT: Test of English as a Foreign Language-Internet-Based Test TOEFL PBT: Test of English as a Foreign, YDS: Yabancı Dil Seviye Tespit Sınavı

Language-Paper-Based Test; TOEFL CBT: Test of English as a Foreign Language-Computer-Based Test; FCE: First Certificate in English;

CAE: Certificate in Advanced English; CPE: Certificate of Proficiency in English

	Quantitative	**Equally Weighted**	**Verbal**
ALES Note			

Computer Skills

Program	**Ability to use**
Microsoft Office Programs	Good
Matlab	Good